

# Exact Renormalized One-Loop Quantum Corrections to Energies of Solitonic Field Configurations

by

Noah Matthew Graham

Submitted to the Department of Physics  
in partial fulfillment of the requirements for the degree of

Doctor of Philosophy

at the

MASSACHUSETTS INSTITUTE OF TECHNOLOGY

June 1999

© Noah Matthew Graham, MCMXCIX. All rights reserved.

The author hereby grants to MIT permission to reproduce and  
distribute publicly paper and electronic copies of this thesis document  
in whole or in part.

Author .....

Department of Physics

April 30, 1999

Certified by .....

Edward Farhi

Professor

Thesis Supervisor

Accepted by .....

Thomas J. Greytak

Associate Department Head for Education

# Exact Renormalized One-Loop Quantum Corrections to Energies of Solitonic Field Configurations

by

Noah Matthew Graham

Submitted to the Department of Physics  
on April 30, 1999, in partial fulfillment of the  
requirements for the degree of  
Doctor of Philosophy

## Abstract

We develop a method for computing exact one-loop quantum corrections to the energies of static classical backgrounds in renormalizable quantum field theories. We use a continuum density of states formalism to construct a regularized Casimir energy in terms of phase shifts and their Born approximations. This method unambiguously incorporates definite counterterms fixed in the standard way by physical renormalization conditions. The result is a robust computation that can be efficiently implemented both numerically and analytically. We carry out such calculations in models of bosons and fermions in one and three dimensions.

Thesis Supervisor: Edward Farhi  
Title: Professor

## Acknowledgments

I would like to thank Professors Edward Farhi and Robert L. Jaffe for being outstanding teachers and collaborators, providing constant support, guidance and encouragement throughout this project. I would also like to thank Benjamin Scarlet for computational help, especially for suggesting a crucial speedup to the calculation of higher order Born approximations. I also would like to thank Sergei Bashinsky, Oliver DeWolfe, Kieran Holland, Tamas Hauer, and Herbert Weigel for many valuable discussions. And my deepest thanks to Nancy, Daniel, and my parents.

# Contents

<b>1</b>	<b>Introduction</b>	<b>6</b>
<b>2</b>	<b><math>\phi^4</math> theory in 1+1 dimensions</b>	<b>11</b>
2.1	Formalism . . . . .	11
2.2	Applications . . . . .	16
2.3	Analytic results . . . . .	20
<b>3</b>	<b>Fermions in one dimension</b>	<b>22</b>
3.1	Formalism . . . . .	22
3.2	Applications . . . . .	26
<b>4</b>	<b>The supersymmetric model in one dimension</b>	<b>30</b>
4.1	Formalism . . . . .	30
4.2	Applications . . . . .	36
4.3	Supersymmetry algebra and the central charge . . . . .	38
<b>5</b>	<b>Scalars in three dimensions</b>	<b>46</b>
5.1	Formalism . . . . .	46
5.2	Computational methods . . . . .	51
5.3	Results . . . . .	53
5.4	Derivative expansion . . . . .	55
<b>6</b>	<b>Fermions in three dimensions</b>	<b>57</b>
<b>7</b>	<b>Conclusions</b>	<b>63</b>

# List of Figures

2-1	The trajectory of $\mathcal{E}[\phi_0]$ in the complex energy plane, with $\mathcal{E}$ in units of $m$ , for $x_0$ increasing from 0 to $\frac{6}{m}$ in steps of $\frac{0.02}{m}$ . Arrows indicate the flow along the real axis. . . . .	18
2-2	Solutions to the equations of motion with a source given by eq. (2.2), as functions of $x$ and $x_0$ in units of $\frac{1}{m}$ . The shaded graph is $\phi_0(x, x_0)$ , which is guaranteed to be a solution by the construction of $J$ . The unshaded graph gives the second solution $\psi_0(x, x_0)$ . (A finer mesh is used for this graph between $x_0 = 0$ and $x_0 = \frac{0.1}{m}$ in order to illustrate its behavior in this region.) . . . . .	19
3-1	Fermion bound state energies as a function of $mx_0$ in units of $m$ . Even parity states are denoted with $\diamond$ and odd parity states with $+$ . . . .	27
3-2	Negative-parity phase shifts as functions of $k/m$ for $x_0 = 2.0, 3.0, 4.0, 5.0, 6.0$ , and $8.0$ . For any finite separation, the phase shift is equal to $\pi$ at $k = 0$ , but as $x_0$ gets larger, the phase shift ascends more and more steeply to $\frac{3\pi}{2}$ . . . . .	28
3-3	Boson bound state squared energies as a function of $mx_0$ in units of $m$ . Symmetric states are denoted with $\diamond$ and antisymmetric states with $+$ . . . .	28
3-4	One-loop fermionic correction to the energy as a function of $x_0$ in units of $m$ . . . . .	29
5-1	One-loop diagrams. . . . .	48
5-2	$\mathcal{E}[h]$ in units of $v$ , for $d = 1$ and $g = 1, 2, 4, 8$ , as a function of $w$ . . . .	54
5-3	$ (\mathcal{E} - \mathcal{E}_{\text{DE}})/(\mathcal{E} - \mathcal{E}_{\text{cl}}) $ for $d = 0.25, g = 4$ , as a function of $w$ . . . . .	56

# Chapter 1

## Introduction

Given a static field configuration in a renormalizable quantum field theory, a natural question to ask is what its energy is. This question is especially relevant in the study of solitons, since they are local minima of the energy. Classically, the energy is simple to calculate from the Lagrangian density of the theory. However, quantization of the theory introduces corrections to this classical result. Such corrections can be expanded as a power series in the coupling constants of the theory, which is equivalent to an expansion in  $\hbar$ .

In this work we will consider the leading quantum corrections to the classical energies of field configurations in a variety of quantum field theories. Since the power of  $\hbar$  counts the number of loops in the diagrammatic expansion of the energy, taking the leading correction will correspond to a one-loop calculation, in which we sum all one-loop diagrams with arbitrary numbers of insertions of the classical background field. This calculation is equivalent to summing the shifts in the  $\frac{1}{2}\hbar\omega$  zero-point energies of all the small fluctuations modes in the presence of the background field. This sum is known as the Casimir energy. As usual in quantum field theory, the result of such a calculation diverges, and we must introduce divergent counterterms that are fixed through a finite set of renormalization conditions. The renormalization conditions define the theory in terms of physical quantities. Our challenge will be to implement such a calculation in a robust, efficient and unambiguous way. In particular, we must isolate the cancellation of divergent quantities without missing any finite contribu-

tions, and we must be sure that we have implemented the renormalization conditions faithfully. Merely “canceling the infinities” is clearly not sufficient when we want to regard a finite result as a physical prediction of a particular theory defined under fixed renormalization conditions.

One application of this method is in coupling of the Higgs sector of the Standard Model to heavy quarks. If we imagine adjusting the Yukawa coupling for a quark doublet so that the quarks’ mass becomes very large, we would expect that when they become sufficiently heavy, they effectively decouple from the theory. However, this cannot be the whole story, since if we simply removed a quark doublet from the Standard Model, we would ruin anomaly cancellation. The resolution of this paradox [1] requires that solitons in the Higgs field carry the quantum numbers of the decoupled fermions. This result suggests a picture in which heavy quarks are realized at small coupling as elementary fermion excitations, and at large coupling as Higgs solitons. In between these two limits, one might then expect to find a hybrid configuration, with the heavy quark tightly bound to a deformation in the Higgs field. To see if this picture is correct, we need to do a variational computation: we must find the field configuration of lowest energy that carries the heavy quark quantum numbers. This application highlights the importance of unambiguously fixing our renormalization conditions and avoiding finite errors in our energy computation. If our renormalization conditions were not fixed precisely, we would effectively be changing the theory as we moved from one background field to another, rendering the variational calculation meaningless.

One could imagine building a Higgs configuration that brings a heavy quark level down from the mass of the quark closer to (or below) zero. The Higgs configuration itself would have an energy cost from the gradient and potential terms in the classical bosonic Hamiltonian. This cost could be balanced by the shift in the “valence” quark energy level, since the quark occupying this state moves to a lower energy. In particular, for strong quark Yukawa coupling (which means large quark mass), and small Higgs self-coupling (which means small Higgs mass), deforming the Higgs field would be favored. However, these two pieces alone do not form a self-consistent

semiclassical calculation. We have included the classical energy along with one part of the leading quantum correction to that energy, the shift in the valence level. We have no justification for ignoring the shifts in all the other quark levels, which contribute at the same order through their zero-point energies. Thus we are forced consider the full Casimir energy in this problem. If we do include the Casimir energy, we obtain a self-consistent semiclassical result. One may doubt the validity of the semiclassical approximation as the coupling gets large, of course, but we will obtain a result that is valid in a well-defined approximation. (In some models, it is also the exact result in a large- $N$  limit [2].)

Although we must compute the full Casimir energy, not just the valence contribution, it is still possible to construct self-consistent approximations to this quantity. Of course, these approximations further restrict the domain of validity of the computation. In particular, if the background field is slowly varying on the scale of the Compton wavelength of the quantum fluctuations, the derivative expansion becomes valid. Indeed, it has been used in models similar to the ones we will consider [2]. However, in both models of heavy quarks and other models we will want to explore, the scale at which the background field varies is precisely the Compton wavelength of the quantum fluctuations, so that all the terms in the derivative expansion will be about the same size, rendering the expansion unreliable. Our approach will be exact to one-loop order.

Central to our technique will be to re-express the Casimir sum in the continuum in terms of phase shifts, using a formalism that originates with Schwinger's work on QED in the presence of strong fields [3]. We will consider only field configurations with some form of spherical symmetry, so that we can use a partial-wave decomposition. In each channel, the difference between the free and interacting density of states is related to the phase shift by

$$\rho(k) = \rho_0(k) + \frac{1}{\pi} \frac{d\delta(k)}{dk} \quad (1.1)$$

which follows from imposing a boundary on the system and then sending the boundary



to infinity, or by more formal S-matrix arguments. In any channel, for any  $k$ , the phase shift is a finite, well-defined, physical quantity. Its analytic structure is well understood in terms of Jost functions, and it can also be rigorously related to the Green's functions and S-matrix of the theory. The sum over continuum modes is then replaced by an integral over the density of states

$$E = \frac{1}{2} \sum_j \omega_j + \frac{1}{2} \int_0^\infty dk \sqrt{k^2 + m^2} \rho(k) \quad (1.2)$$

in which the bound states are still included explicitly. This mathematical artillery leads to several important properties of the phase shifts:

- We can expand the phase shifts as a Born series in the strength of the potential. This expansion is in exact correspondence with the expansion of the full propagator of the theory in terms of the free propagators connecting insertions of the potential. The Born expansion also has simple behavior at large  $k$  and becomes more and more accurate in this limit, which will enable us to use it as a regulator of ultraviolet divergences.
- The phase shifts track level crossings, ensuring a consistent counting of modes as states become bound. This property allow us to avoid a serious problem we would encounter if we put the system in a box, because in that case we would have a hard time ensuring that we have kept the appropriate number of modes when computing the Casimir energy and the contribution of the counterterms. Missing even one mode in the Casimir sum will lead to a drastic change in the final answer; although such an error is small compared to the leading (divergent) behavior of the sum, the leading behavior is cancelled by the counterterms. The final answer is generically of the same order as a typical energy level. Our key tool here will be Levinson's theorem, which relates the phase shift at  $k = 0$  to the number of bound states.
- The phase shifts and their Born approximations are simple, robust quantities amenable to both numerical and analytic calculation. We will see that they

enable us to replace the cancellations of large quantities, the Casimir energy against the counterterms, by the much more manageable cancellation of exact phase shift against Born approximation. Many cases will in the end be tractable only numerically, but we will also find that numerical analysis will also shed light on analytic results by allowing us to continuously interpret between a trivial configuration and one that can be solved analytically.

- The absence of boundaries will allow us to avoid spurious contributions from artificial boundary conditions. This property will be especially useful in models with fermions.
- In principle, phase shifts can even be computed in fractional dimensions, since they obey a simple radial differential equation that depends analytically on the dimension of space. In particular, the first Born approximation the bosonic phase shifts can be analytically calculated in arbitrary dimensions terms of generalized Bessel functions. This result agrees exactly with the result one would find for the corresponding tadpole graph evaluated in dimensional regularization.

Much of this work originally appeared in [4].

# Chapter 2

## $\phi^4$ theory in 1+1 dimensions

We will begin with examples in 1+1 dimensions. The study of exactly soluble 1+1 dimensional problems has yielded many insights into fundamental problems in field theory. Other 1+1 dimensional problems cannot be solved exactly, making it important to understand which properties of exact results will generalize to more generic cases and which are special to the exactly soluble cases. The renormalization process is simpler in one dimension than it is in three, since theories in lower dimensions are less divergent, but it still must be approached carefully. Indeed, we will find that the one dimensional problem actually contains additional subtleties not present in higher dimensions.

### 2.1 Formalism

We will consider a standard  $\phi^4$  theory with spontaneous symmetry breaking and a source  $J(x)$ . The action is

$$S[\phi] = \frac{m^2}{\lambda} \int \left( \frac{1}{2} (\partial_\mu \phi)^2 - \frac{m^2}{8} (\phi^2 - 1)^2 - J(x)\phi + \mathcal{L}_{\text{ct}} \right) d^2x \quad (2.1)$$

where  $\mathcal{L}_{\text{ct}}$  is the counterterm Lagrangian. Our metric has  $g_{tt} = -g_{xx} = 1$ . We have rescaled the field  $\phi$  somewhat unconventionally in order to make explicit the correspondence between the powers of  $\lambda$  and the powers of  $\hbar$ , which we have set equal

to 1. Classical terms will go as  $\frac{1}{\lambda}$ , the one-loop terms we compute will go as  $\lambda^0$ , and higher loops will contribute with higher powers of  $\lambda$ . The mass of fluctuations around the trivial vacua  $\phi(x) = \pm 1$  is  $m$ , and we define the potential  $U(\phi) = \frac{m^2}{8}(\phi^2 - 1)^2$ .

We consider a fixed field configuration  $\phi_0(x)$ . Initially we will assume that  $\phi_0(x) = \phi_0(-x)$ , which restricts us to the topologically trivial sector of the theory. However, we will see that our method works equally well for the case of  $\phi_0(x) = -\phi_0(-x)$ , so that in fact we can deal with configurations with any topology as long as  $U(\phi_0)$  has reflection symmetry. We adjust the source so that  $\phi_0$  is a stationary point of the action, which means that  $J$  then solves the equation

$$J(x) = \frac{d^2\phi_0}{dx^2} - \frac{1}{2}m^2(\phi_0^3 - \phi_0). \quad (2.2)$$

We can always solve this equation for  $J$ , but there is no guarantee that the  $J$  we find will always correspond to a unique  $\phi_0$ , as we will see later. If  $\phi_0$  is a solution to the equations of motion, of course the source will be zero.

We would like to consider the leading quantum correction to the classical energy of this configuration, which we can represent as the sum of the zero-point energies of the normal modes of small oscillations around  $\phi_0$ . Writing  $\phi = \phi_0 + \eta$ , the normal modes are solutions of

$$-\frac{d^2\eta}{dx^2} + (V(x) + m^2)\eta = \omega^2\eta \quad (2.3)$$

with  $V(x) = U''(\phi_0(x)) - m^2 = \frac{3}{2}m^2(\phi_0^2(x) - 1)$ . The quantum change in energy in going from the trivial vacuum to  $\phi_0(x)$  is then

$$\mathcal{E}[\phi_0] = \frac{1}{2}(\sum \omega - \sum \omega_0) + \mathcal{E}_{\text{ct}} = \Delta E + \mathcal{E}_{\text{ct}} \quad (2.4)$$

where  $\omega_0$  are the free solutions (with  $\phi_0^2(x) = 1$ ), and  $\mathcal{E}_{\text{ct}}$  is the contribution from the counterterms.

Note that it is possible that some of the values of  $\omega^2$  will be negative, so that in these directions our stationary point is a local maximum rather than a minimum of the action. These solutions will add an imaginary part to the energy, which we

can interpret via analytic continuation as giving the decay rates through the unstable modes [5]. If there is a direction in field space in which small oscillations lower the energy, we should be able to keep going in that direction and arrive at a lower minimum. Later, we will see explicitly that the appearance of unstable modes coincides with the existence of a second solution to the  $\phi_0$  equation with the same  $J$  and lower energy.

We would like to rewrite the sum over zero-point energies as an integral over phase space of the product of the energy and the density of states. We can then break this integral into a sum over bound states and an integral over a continuum, representing the latter in terms of phase shifts. In order to do so, however, we must review the peculiarities of Levinson's theorem in one dimension. For more details on these results see [6] and [7]. For a symmetric  $V(x)$ , we can divide the continuum states into symmetric and antisymmetric channels, and then calculate the phase shift as a function of  $k$  separately for each channel, where  $\omega^2 = k^2 + m^2$ . The antisymmetric channel is completely equivalent to the  $l = 0$  case in three dimensions, so we have

$$\delta_A(0) = n_A \pi \quad (2.5)$$

where  $n_A$  is the number of antisymmetric bound states. However, we must be careful in dealing with the special case of a state exactly at  $k = 0$ . In this case the solution to eq. (2.3) with  $k = 0$  goes asymptotically to a constant as  $x \rightarrow \infty$ , as opposed to the generic case where the  $k = 0$  solution goes to a constant plus linear terms in  $x$ . Just as in the  $l = 0$  case in three dimensions, this state contributes  $\frac{1}{2}$  to  $n_A$ . We will refer to such states as “half-bound states.”

In the symmetric channel, Levinson's theorem becomes

$$\delta_S(0) = n_S \pi - \frac{\pi}{2} \quad (2.6)$$

where a bound state at  $k = 0$  contributes  $\frac{1}{2}$  to  $n_S$ , just as in the antisymmetric case. We can see the importance of getting the half-bound states right by looking at the free case: the phase shift is zero everywhere, and the right-hand side is zero because

the free case has a half-bound state (the wavefunction  $\psi = \text{constant}$ ). The situation is equally subtle for reflectionless potentials, all of which have half-bound states and  $\delta_S(0) + \delta_A(0)$  equal to an integer times  $\pi$ .

We are now ready to rewrite the change in the zero-point energies in terms of phase shifts. Letting  $E_j$  be the bound state energies (again with  $k = 0$  bound states contributing with a  $\frac{1}{2}$ ),  $\rho(k)$  be the density of states and  $\rho_0(k)$  be the free density of states, we have

$$\begin{aligned}\Delta E &= \frac{1}{2} \sum_j E_j - \frac{m}{4} + \int_0^\infty \frac{dk}{2\pi} \omega(k) (\rho(k) - \rho_0(k)) \\ &= \frac{1}{2} \sum_j E_j - \frac{m}{4} + \int_0^\infty \frac{dk}{2\pi} \omega(k) \frac{d}{dk} (\delta_A(k) + \delta_S(k))\end{aligned}\quad (2.7)$$

where  $\omega(k) = \sqrt{k^2 + m^2}$  and we have used

$$\rho(k) = \rho_0(k) + \frac{1}{\pi} \frac{d}{dk} (\delta_A(k) + \delta_S(k)). \quad (2.8)$$

Note that the  $\frac{m}{4}$  term subtracts the contribution of the free half-bound state.

Eq. (2.7) is divergent (the phase shifts fall as  $\frac{1}{k}$  for  $k \rightarrow \infty$ ), which is what we should expect since it includes the divergent contribution from the tadpole graph without the divergent contribution from the counterterms that cancels it.

To avoid infrared problems later, we first use Levinson's theorem to compute the change in particle number, which is given by

$$0 = \sum_j 1 + \int_0^\infty \frac{dk}{\pi} \frac{d}{dk} (\delta_A(k) + \delta_S(k)) - \frac{1}{2} \quad (2.9)$$

where again, half-bound states are counted with a  $\frac{1}{2}$  in the sum over  $j$  and the  $-\frac{1}{2}$  comes from the contribution of the free half-bound state. Subtracting  $\frac{m}{2}$  times this equation from eq. (2.7), we have

$$\Delta E = \frac{1}{2} \sum_j (E_j - m) + \int_0^\infty \frac{dk}{2\pi} (\omega(k) - m) \frac{d}{dk} (\delta_A(k) + \delta_S(k)). \quad (2.10)$$

Next, we subtract the first Born approximation to eq. (2.10), which corresponds exactly to the tadpole graph. We must then add it back in using ordinary renormalized perturbation theory. However, in 1+1 dimensions we can adopt the simple renormalization condition that the counterterms cancel the tadpole graph and perform no additional finite renormalizations beyond this cancellation. With this choice, there is then nothing to add back in.

The first Born approximation is given by

$$\begin{aligned}\delta_S^{(1)}(k) &= -\frac{1}{k} \int_0^\infty V(x) \cos^2 kx \, dx \\ \delta_A^{(1)}(k) &= -\frac{1}{k} \int_0^\infty V(x) \sin^2 kx \, dx.\end{aligned}\tag{2.11}$$

Notice that the sum of these two depends on  $V(x)$  only through the quantity  $\langle V \rangle = \int_0^\infty dx V(x)$ , so we can indeed cancel the tadpole contribution with available counterterms.

Subtracting the first Born approximation, we have

$$\mathcal{E}[\phi_0] = \frac{1}{2} \sum_j (E_j - m) + \int_0^\infty \frac{dk}{2\pi} (\omega(k) - m) \frac{d}{dk} (\delta_A(k) + \delta_S(k) + \frac{\langle V \rangle}{k}).\tag{2.12}$$

Since the Born approximation becomes exact at large  $k$ , the  $\frac{\langle V \rangle}{k}$  term exactly cancels the leading  $\frac{1}{k}$  behavior of the phase shift at large  $k$ . As a result, this integral is completely finite and well-defined, since the integrand goes like  $\frac{1}{k^2}$  for  $k \rightarrow \infty$  and goes to a constant at  $k = 0$ . We must find such a result, since in 1+1 dimensions eliminating the tadpole is sufficient to render the theory finite.

In particular, we are free to integrate by parts, giving an expression that will be easier to deal with computationally,

$$\mathcal{E}[\phi_0] = \frac{1}{2} \sum_j (E_j - m) - \int_0^\infty \frac{dk}{2\pi} \frac{k}{\omega(k)} (\delta_A(k) + \delta_S(k) + \frac{\langle V \rangle}{k}).\tag{2.13}$$

Our use of Levinson's theorem to regularize  $\Delta E$  in the infrared (replacing eq. (2.7) by eq. (2.10)) avoided a subtlety of the Born approximation in one dimension that

does not occur in higher dimensions: as  $k \rightarrow 0$ , the symmetric contribution from eq. (2.11) introduces a spurious infrared divergence, since it goes like  $\frac{1}{k}$ . (Each higher dimension adds a power of  $k$  near  $k = 0$ . We can see this in the Feynman diagram calculation, where these powers of  $k$  come from the measure.)

## 2.2 Applications

We can now use eq. (2.13) to calculate quantum energies for specific field configurations. Knowing that our model has a “kink” soliton solution  $\phi_0(x) = \tanh \frac{mx}{2}$ , we will consider a family of field configurations that continuously interpolate between the trivial vacuum and a soliton/antisoliton pair,

$$\phi_0(x, x_0) = \tanh \frac{m}{2}(x + x_0) - \tanh \frac{m}{2}(x - x_0) - 1, \quad (2.14)$$

with  $2x_0$  measuring approximately the separation between the soliton and antisoliton. Unlike the kink, these configurations are not solutions of the equations of motion, except in the  $x_0 \rightarrow 0$  and  $x_0 \rightarrow \infty$  limits. Thus we will need to introduce a source that will vanish in these limits, and we must analyze the stability questions we raised earlier.

For  $x_0$  very small, we simply have a small attractive perturbation from the trivial vacuum held in place by a small source, which we would not expect to introduce any instabilities. In terms of the scattering problem, for small  $x_0$ , the potential is too weak to bind a state with a binding energy greater than  $m$ , which would give an imaginary eigenvalue.

For  $x_0$  very large, we have a widely separated soliton/antisoliton pair. We know from translation invariance that a single soliton has a mode with  $\omega^2 = 0$ . Since this zero mode corresponds to a nodeless wavefunction, it is the lowest energy mode. The soliton/antisoliton pair has two translation modes that will mix, giving a symmetric eigenstate with a slightly lower energy and an antisymmetric eigenstate with a slightly higher energy. Thus we expect to find a single symmetric mode with  $\omega^2 < 0$ , which



will contribute an imaginary part to  $\mathcal{E}[\phi_0]$ . The imaginary part gives the rate for our field configuration to decay through this mode toward the trivial vacuum. As  $x_0 \rightarrow \infty$ , we should find that the imaginary part goes to zero, and the real part goes to twice the energy of a single soliton, which we compute exactly below.

According to this analysis, there should be a finite, nonzero value of  $x_0$  where the imaginary eigenvalue first appears. At this point, the field becomes unstable with respect to small perturbations in some direction in field space. Therefore, the energy must have a lower minimum that we can reach by moving in that direction. This configuration  $\psi_0(x, x_0)$  is a second stationary point of the action with the same source, which crosses  $\phi_0$  at the value of  $x_0$  where the imaginary part for the energy appears. (For smaller values of  $x_0$ , this solution still exists but has higher energy.) In terms of the scattering problem, this crossing appears when the potential has a bound state with  $\omega^2 = 0$ . We can identify this state explicitly: since  $\phi_0$  and  $\psi_0$  satisfy eq. (2.2) with the same  $J$ , as we approach the crossing, the wavefunction  $\eta(x) = \psi_0(x, x_0) - \phi_0(x, x_0)$  becomes a solution to eq. (2.3) with  $\omega^2 = 0$ .

We have carried out this computation numerically, and find results that agree with all of these expectations. To compute the antisymmetric phase shift, we will parameterize the wavefunction as

$$\eta(x) = e^{-ikx} - e^{ikx} e^{2i\beta(x)} \quad (2.15)$$

where  $\beta(x)$  is an arbitrary complex function. Solving the differential equation for  $\eta(x)$  subject to  $\eta(0) = 0$ , we find

$$\delta_A(k) = -2 \operatorname{Re} \beta(k, 0) \quad (2.16)$$

where  $\beta(k, x)$  is 0 at  $x = \infty$  and satisfies

$$-i\beta'' + 2k\beta' + 2(\beta')^2 + \frac{1}{2}V(x) = 0, \quad (2.17)$$

with prime denoting differentiation with respect to  $x$ . To obtain the symmetric phase

shift, we can follow the same derivation, but instead of imposing  $\eta(0) = 0$  on the wavefunction, we instead impose  $\eta'(0) = 0$ , giving

$$e^{2i\delta_S} = \frac{e^{2i\beta}}{e^{-2i\beta^*}} \frac{k + 2\beta'}{k + 2\beta'^*} \quad (2.18)$$

with  $\beta$  the same as above, so that

$$\delta_S(k) = \delta_A(k) - \tan^{-1}\left(\frac{2 \operatorname{Im} \beta'(k, 0)}{k + 2 \operatorname{Re} \beta'(k, 0)}\right). \quad (2.19)$$

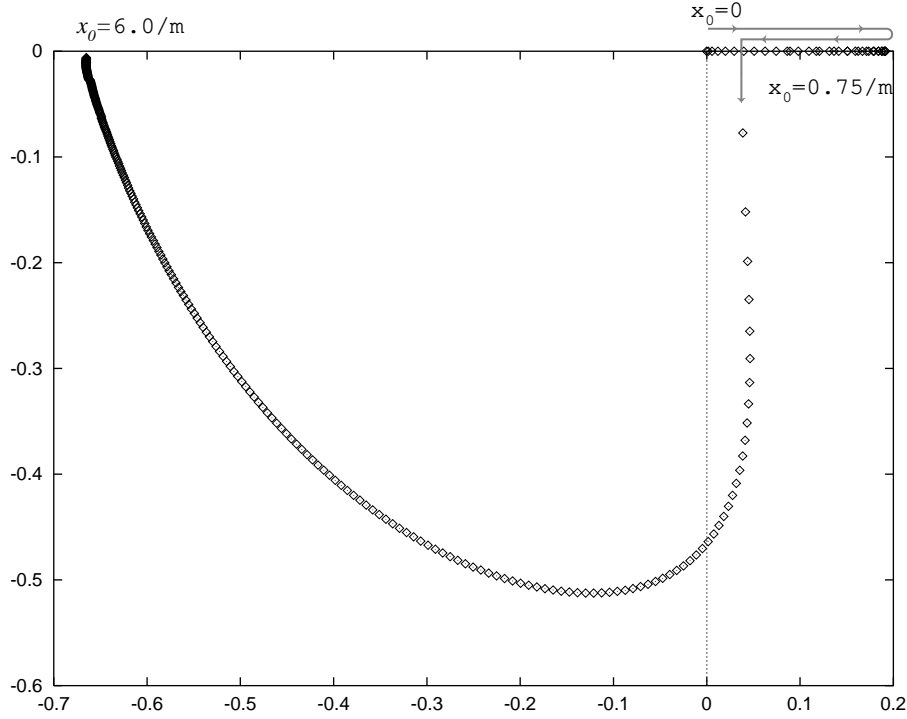


Figure 2-1: The trajectory of  $\mathcal{E}[\phi_0]$  in the complex energy plane, with  $\mathcal{E}$  in units of  $m$ , for  $x_0$  increasing from 0 to  $\frac{6}{m}$  in steps of  $\frac{0.02}{m}$ . Arrows indicate the flow along the real axis.

Fig. 2-1 shows the trajectory of  $\mathcal{E}[\phi_0]$  in the complex plane as a parametric function of  $x_0$ , starting from the origin at  $x_0 = 0$ . When  $x_0 \approx \frac{0.75}{m}$ , a single imaginary eigenvalue appears and  $\mathcal{E}[\phi_0]$  leaves the real axis. For  $x_0$  large,  $\mathcal{E}[\phi_0]$  approaches  $2(\frac{1}{4\sqrt{3}} - \frac{3}{2\pi})$ , twice the standard result for a single soliton. The actual trajectory of  $\mathcal{E}[\phi_0]$  has little significance, since it depends in detail on the functional form of

$\phi(x, x_0)$ . However, the general features — beginning at the origin, moving up the real axis, out into the complex plane, and finally asymptotically to the real two-solution value — are characteristics of any  $\phi_0$  that begins at the vacuum and ends at a well separated kink and antikink.

Fig. 2-2 shows  $\phi_0(x, x_0)$  and the second solution to the equations of motion with the same  $J$ ,  $\psi_0(x, x_0)$ .  $\psi_0$  goes to the trivial vacuum as  $x_0 \rightarrow \infty$ , and becomes a widely separated soliton/antisoliton pair as  $x_0 \rightarrow 0$ , crossing  $\phi_0$  at  $x_0 \approx 0.75$ . For  $x_0$  below this value,  $\phi_0$  has lower classical energy, while above this point,  $\psi_0$  has lower classical energy, and this crossing appears precisely where the imaginary eigenvalue appears in the small oscillations spectrum.

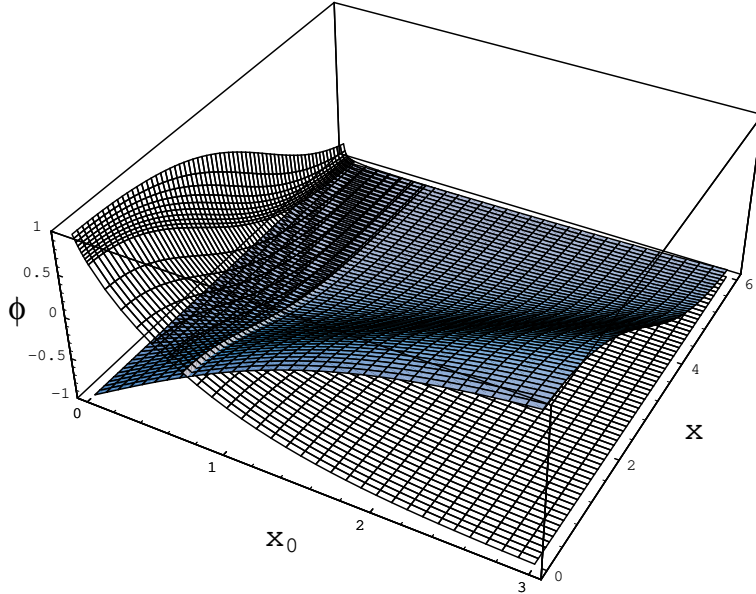


Figure 2-2: Solutions to the equations of motion with a source given by eq. (2.2), as functions of  $x$  and  $x_0$  in units of  $\frac{1}{m}$ . The shaded graph is  $\phi_0(x, x_0)$ , which is guaranteed to be a solution by the construction of  $J$ . The unshaded graph gives the second solution  $\psi_0(x, x_0)$ . (A finer mesh is used for this graph between  $x_0 = 0$  and  $x_0 = \frac{0.1}{m}$  in order to illustrate its behavior in this region.)

Through this continuous deformation from the trivial vacuum, we have arrived at a widely separated soliton/antisoliton pair, which we can now separate into independent configurations with nontrivial topology. These configurations are exactly soluble, so we will be able to study them analytically. However, our method does not rely on

having an analytic solution, so we could numerically calculate the energy of a generic field configuration with nontrivial topology using the same techniques.

## 2.3 Analytic results

In one dimensional quantum mechanics, potentials of the form

$$V_\ell(x) = -\frac{\ell+1}{\ell}m^2\text{sech}^2\left(\frac{mx}{\ell}\right) \quad (2.20)$$

with  $\ell$  an integer are exactly soluble and reflectionless. Their properties are summarized in Appendix A. The single soliton solution in our model,  $\phi_0(x) = \tanh \frac{mx}{2}$ , corresponds to  $V(x) = -\frac{3}{2}m^2\text{sech}^2\frac{mx}{2}$ , the  $\ell = 2$  case of this family. (The sine-Gordon soliton corresponds to the  $\ell = 1$  case.) For a reflectionless potential,  $\delta_S(k) = \delta_A(k)$ ; to reconcile this equality with Levinson's theorem in the symmetric and antisymmetric channels,  $V_l(x)$  must have a half-bound state. (We saw this behavior already for the  $\ell = 0$  case, the free particle.) We also note that although  $\delta_S = \delta_A$ ,  $\delta_S^{(1)} \neq \delta_A^{(1)}$ , so the renormalized contributions from the symmetric and antisymmetric channels are not the same. In addition, the bound state contributions will also be unequal.

For our case, the exact result for the phase shift is

$$\delta_S(k) = \delta_A(k) = -\tan^{-1} \frac{3mk}{m^2 - 2k^2}, \quad (2.21)$$

where the branch of the arctangent is chosen so that the phase shift is continuous and goes to zero for  $k \rightarrow \infty$ . The Born approximation is

$$\delta_S^{(1)}(k) + \delta_A^{(1)}(k) = \frac{3m}{k}. \quad (2.22)$$

There are three bound states: a translation mode with  $E = 0$ , a state with  $E = \frac{m\sqrt{3}}{2}$ , and a half-bound state with  $E = m$ . Using eq. (2.12) or eq. (2.13) we find

$$\mathcal{E}[\phi_0] = m\left(\frac{1}{4\sqrt{3}} - \frac{3}{2\pi}\right) \quad (2.23)$$

in agreement with [11], [10], and the mode number cutoff method in [8].

We can calculate the energy of the soliton of the sine-Gordon model using the same methods. In this model, the  $\frac{m^2}{4}(\phi^2 - 1)^2$  potential is replaced by

$$U(\phi) = m^2(\cos \phi - 1) \quad (2.24)$$

which has soliton (anti-soliton) solutions

$$\phi_0 = 4 \tan^{-1}(\exp(\mp m(x - x_0))). \quad (2.25)$$

The phase shift is

$$\delta_S(k) = \delta_A(k) = \tan^{-1} \frac{m}{k} \quad (2.26)$$

with Born approximation

$$\delta_S^{(1)}(k) + \delta_A^{(1)}(k) = \frac{2m}{k}. \quad (2.27)$$

The bound states are just the translation mode at  $E = 0$  and the half-bound state at  $E = m$ , giving

$$\mathcal{E}[\phi_0] = -\frac{m}{\pi} \quad (2.28)$$

again agreeing with the established results.

# Chapter 3

## Fermions in one dimension

We next extend our methods by adding fermions. We will see that our techniques extend cleanly and unambiguously to this case, and deal elegantly with the subtleties of boundary conditions.

### 3.1 Formalism

We consider a Majorana fermion  $\Psi$  interacting with a scalar background field  $\phi$ , with the classical Lagrangian density

$$\mathcal{L} = \frac{m^2}{2\lambda} \left( i\bar{\Psi}\not{\partial}\Psi - m\phi\bar{\Psi}\Psi + \mathcal{L}_\phi \right) \quad (3.1)$$

where  $\mathcal{L}_\phi$  is the Lagrangian density for the  $\phi$  background field, which we will take to be the same as in the last section, with the same soliton solutions. We note that choosing the Lagrangian density in this way causes the bosonic and fermionic degrees of freedom to be related by supersymmetry for a background field that is a solution to the equations of motion (such as a single soliton or an infinitely separated soliton/antisoliton pair). In this section, we will use this property only because we will find it instructive to compare the bosonic and fermionic small oscillations spectra. In the next section, we will consider the full supersymmetric model.

The one-loop corrections to the energy due to fermionic fluctuations will be

given by the appropriately renormalized sum of the zero-point energies,  $-\frac{1}{2}\omega$ , of the fermionic small oscillations. The spectrum of fermionic small oscillations in a background  $\phi_0(x)$  is given by the Dirac equation,

$$\gamma^0 \left( -i\gamma^1 \frac{d}{dx} + V_F(x) \right) \psi_k(x) = \omega_k^F \psi_k(x) \quad (3.2)$$

where  $V_F(x) = m\phi_0(x)$  is the fermionic potential and  $k = \pm\sqrt{\omega^2 - m^2}$  is the momentum labeling the scattering states.

We will choose the convention  $\gamma^0 = \sigma_2$  and  $\gamma^1 = i\sigma_3$  so that the Majorana condition becomes simply  $\Psi^* = \Psi$ . We note that since our Lagrangian is  $CP$  invariant, all of our results for the spectrum of a Majorana fermion can be extended to a Dirac fermion simply by doubling.

Again, we will need to find the phase shifts. We can solve for the phase shifts of any fermionic potential  $V_F(x)$  that satisfies  $V_F(x) = V_F(-x)$  and  $V_F(x) \rightarrow m$  as  $x \rightarrow \pm\infty$  by generalizing the methods of the previous section. This form will be useful for considering our example of a sequence of background field configurations that continuously interpolates between the trivial vacuum and a widely separated soliton-antisoliton pair. In the limit of infinite separation, the phase shift for the pair goes to twice the result for a single soliton. For comparison, we also do the computation for a single soliton directly below.

We define the parity operator acting on fermionic states as  $P = \Pi\gamma^0$ , where  $\Pi$  sends  $x \rightarrow -x$ .  $P$  commutes with the Hamiltonian, so parity is a good quantum number. As a result, we can separate the small oscillations into positive and negative parity channels, now restricted to  $k > 0$  in the continuum.

We parameterize the fermion solutions by

$$\chi_1(x) = \begin{pmatrix} e^{i\nu(x)} \\ ie^{i\zeta(x)}e^{i\theta} \end{pmatrix} e^{ikx} \quad \text{and} \quad \chi_2(x) = \begin{pmatrix} e^{-i\nu(x)^*} \\ ie^{-i\zeta(x)^*}e^{-i\theta} \end{pmatrix} e^{-ikx} \quad (3.3)$$

where  $\theta = \tan^{-1} \frac{k}{m}$  and  $\nu$  and  $\zeta$  are complex functions of  $x$ . We then find the phase

shift in each channel  $\delta^\pm(k)$  by solving eq. (3.2) subject to the boundary conditions

$$\psi^\pm(0) \propto \begin{pmatrix} 1 \\ \pm i \end{pmatrix} \quad (3.4)$$

giving the phase shift as

$$\psi^\pm(0) = e^{\frac{i\theta}{2}} \chi_2(0) \pm e^{2i\delta^\pm(k)} e^{-\frac{i\theta}{2}} \chi_1(0). \quad (3.5)$$

Our boundary conditions assure that the wavefunctions  $\psi^\pm$  are eigenstates of the parity operator with eigenvalues  $\pm 1$ . We obtain

$$\begin{aligned} \delta^+(k) &= -\text{Re } \nu(0) + \frac{\theta}{2} + \frac{1}{2i} \log \frac{Y-1}{1-Y^*} \\ \delta^-(k) &= -\text{Re } \nu(0) + \frac{\theta}{2} + \frac{1}{2i} \log \frac{1+Y}{1+Y^*} \end{aligned} \quad (3.6)$$

where  $Y = \frac{1}{\omega}(V_F(0) - ik + i\nu'(0)^*)$  and  $\nu(x)$  satisfies

$$-i\nu(x)'' + \nu'(x)^2 + 2k\nu'(x) + V_F(x)^2 - V_F(x)' - m^2 = 0 \quad (3.7)$$

with the boundary condition that  $\nu(x)$  and  $\nu'(x)$  vanish at infinity. The total phase shift is given by summing the phase shifts in each channel,  $\delta_F(k) = \delta^+(k) + \delta^-(k)$ .

Again, once we know the phase shifts, Levinson's theorem tells us how many bound states there will be. It works exactly the same way as in the bosonic case [7]: In the odd parity channel, the number of bound states  $n_-$  is given by

$$\delta^-(0) = \pi n_- \quad (3.8)$$

while in the even parity channel the number of bound states  $n_+$  is given by

$$\delta^+(0) = \pi(n_+ - \frac{1}{2}). \quad (3.9)$$

One can derive this result either by the same Jost function methods used in the boson



case, or by observing that at small  $k$ , the nonrelativistic approximation becomes valid so the bosonic results carry over directly. As in the boson case, for a particular potential there may exist a  $k = 0$  state in either of the two channels whose Dirac wavefunction goes to a constant spinor as  $x \rightarrow \pm\infty$ . (Generically, for  $k = 0$  the components of the Dirac wavefunction go to straight lines as  $x \rightarrow \pm\infty$ , but not lines with zero slope.) Just as in the bosonic case, such threshold states (which we will again call “half-bound states”) should be counted with a factor of  $\frac{1}{2}$  in Levinson’s theorem.

Given the phase shifts and bound state energies, we can calculate the one-loop fermionic correction to the energy. We continue to work in the simple renormalization scheme in which we add a counterterm proportional to  $\phi^2 - 1$ , and perform no further renormalizations. The counterterm is fixed by requiring that the tadpole graph cancel. As in the bosonic case, we use the density of states

$$\rho(k) = \rho_0(k) + \frac{1}{\pi} \frac{d\delta_F(k)}{dk} \quad (3.10)$$

to write

$$\mathcal{E}[\phi_0] = -\frac{1}{2} \sum_j \omega_j - \int_0^\infty \frac{dk}{2\pi} \omega \frac{d\delta_F(k)}{dk} + \mathcal{E}_{\text{ct}} \quad (3.11)$$

where  $\omega = \sqrt{k^2 + m^2}$  and the sum over  $j$  counts bound states with appropriate factors of  $\frac{1}{2}$  as discussed above. Next, we use eq. (3.8) and eq. (3.9) to rewrite this expression as

$$\mathcal{E}[\phi_0] = -\frac{1}{2} \sum_j (\omega_j - m) - \int_0^\infty \frac{dk}{2\pi} (\omega - m) \frac{d\delta_F(k)}{dk} + \mathcal{E}_{\text{ct}}. \quad (3.12)$$

In terms of the shifted field  $\phi - 1$ , the (divergent) contribution from the tadpole graph is given by the leading Born approximation to  $\delta_F$ . A corresponding divergence related by  $\phi \rightarrow -\phi$  symmetry appears in the second-order diagram. To subtract the tadpole graph, we subtract the leading Born approximation in  $V_F - m$ . In order to maintain the  $\phi \rightarrow -\phi$  symmetry, we also subtract the corresponding piece of the second-order diagram by subtracting the part of the second Born approximation related by the symmetry. Since we have chosen the counterterm to exactly cancel

these subtractions, there is nothing to add back in. Thus we have

$$\mathcal{E}[\phi_0] = -\frac{1}{2} \sum_j (\omega_j - m) - \int_0^\infty \frac{dk}{2\pi} (\omega - m) \frac{d}{dk} (\delta_F(k) - \delta_F^{(1)}(k)) \quad (3.13)$$

where

$$\delta^{(1)}(k) = -\frac{1}{k} \int \left( V_F(x)^2 - V_F(x)' - m^2 \right) dx \quad (3.14)$$

which can also be obtained numerically by iterating eq. (3.7). For the soliton/antisoliton pair, the contribution from  $V'(x)$  vanishes since it is a total derivative, so that again our subtraction is indeed proportional to  $\phi^2 - 1$ .

## 3.2 Applications

We continue to study a sequence of background fields labeled by a parameter  $x_0$  that continuously interpolates from the trivial vacuum  $\phi(x) = 1$  at  $x_0 = 0$  to a widely separated soliton/antisoliton pair at  $x_0 \rightarrow \infty$ ,

$$\phi(x, x_0) = 1 + \tanh \frac{m(x - x_0)}{2} - \tanh \frac{m(x + x_0)}{2}. \quad (3.15)$$

Fig. 3-1 shows the fermionic bound state energies as a function of  $x_0$ . In the limit  $x_0 \rightarrow \infty$  two bound states approach energy  $m\frac{\sqrt{3}}{2}$ . These are simply the odd and even parity combinations of the single soliton bound state at  $m\frac{\sqrt{3}}{2}$ . The third (positive parity) bound state approaches  $\omega = 0$  where the single soliton also has a bound state, but there is only *one* such state (with  $\omega > 0$ ). Thus for a single soliton we must thus count the zero mode with a factor of  $\frac{1}{2}$ . We will see this result analytically below.

For any finite  $x_0$ , Levinson's theorem holds without subtleties; there are no states that require factors of  $\frac{1}{2}$ . Thus for a large but finite  $x_0$ , we find

$$\begin{aligned} \delta^+(0) &= \frac{3\pi}{2} \\ \delta^-(0) &= \pi \end{aligned} \quad (3.16)$$

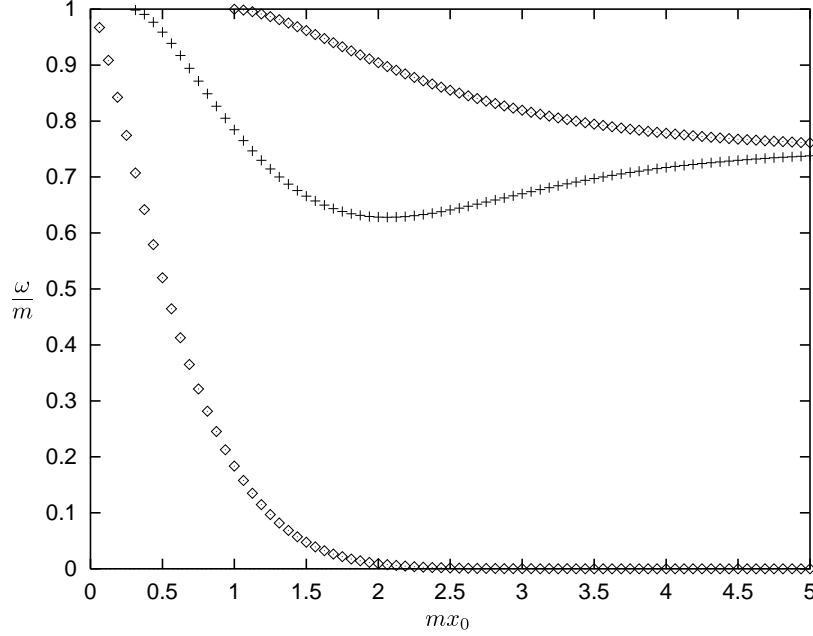


Figure 3-1: Fermion bound state energies as a function of  $mx_0$  in units of  $m$ . Even parity states are denoted with  $\diamond$  and odd parity states with  $+$ .

consistent with having two positive parity and one negative parity bound states (see Fig. 3-1). In the limit  $x_0 \rightarrow \infty$ , an even parity “half-bound” threshold state enters the spectrum at  $\omega = m$  just as in the bosonic case. Also, in this limit, the lowest (positive parity) mode approaches  $\omega = 0$ , and is only counted as a  $\frac{1}{2}$  as described above. Finally, a negative parity mode enters the spectrum from below, also to be weighted by  $\frac{1}{2}$ .

Thus the net change is to add half of a negative parity state, which via Levinson’s theorem requires the phase shift  $\delta^-(0)$  to jump from  $\pi$  to  $\frac{3\pi}{2}$  as  $x_0 \rightarrow \infty$ . This jump occurs by the same continuous but nonuniform process as in all cases where a new state gets bound, which is illustrated in Fig. 3-2. Just as in the bosonic case, in the limit of infinite separation the potential we have chosen becomes reflectionless, which requires  $\delta^+(k) = \delta^-(k)$ .

To contrast the behavior of the zero modes, Fig. 3-3 shows  $\omega^2$  for the bound states of the bosonic small oscillations. Because we have chosen the bosonic potential to be consistent with supersymmetry, the bosonic and fermionic spectra are related. Again as  $x_0 \rightarrow \infty$  the bound state energies approach those of the single soliton, and the

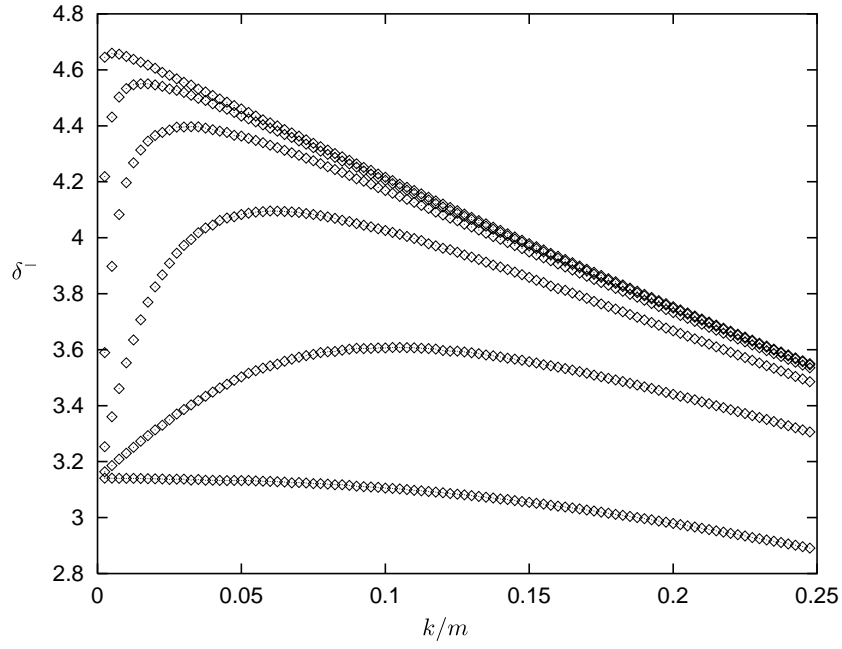


Figure 3-2: Negative-parity phase shifts as functions of  $k/m$  for  $x_0 = 2.0, 3.0, 4.0, 5.0, 6.0$ , and  $8.0$ . For any finite separation, the phase shift is equal to  $\pi$  at  $k = 0$ , but as  $x_0$  gets larger, the phase shift ascends more and more steeply to  $\frac{3\pi}{2}$ .

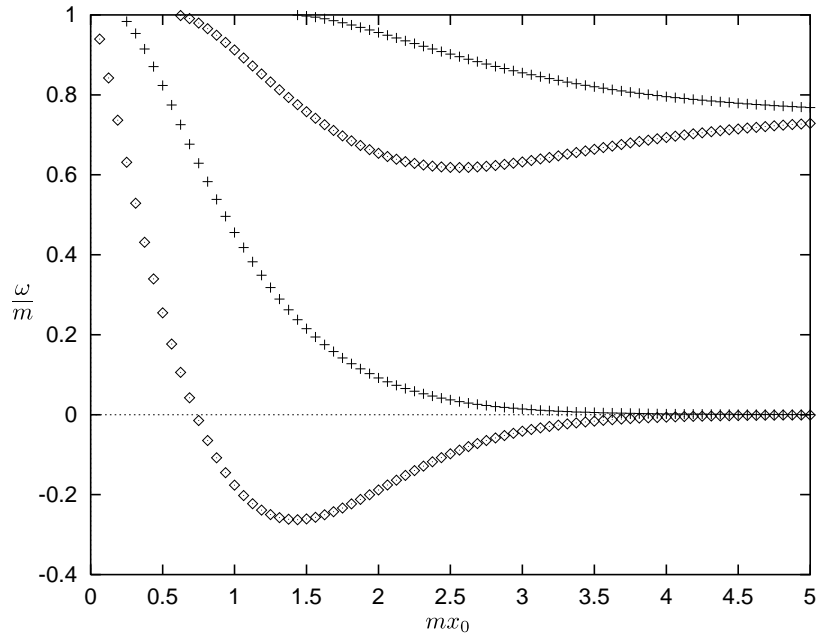


Figure 3-3: Boson bound state squared energies as a function of  $mx_0$  in units of  $m$ . Symmetric states are denoted with  $\diamond$  and antisymmetric states with  $+$ .

wavefunctions are formed from the odd and even combinations of the wavefunctions for the single soliton. However, we see that in the boson case both the mode at  $m\frac{\sqrt{3}}{2}$  and the mode at  $\omega = 0$  are doubled, so there is no factor of  $\frac{1}{2}$  in counting the bosonic zero modes.

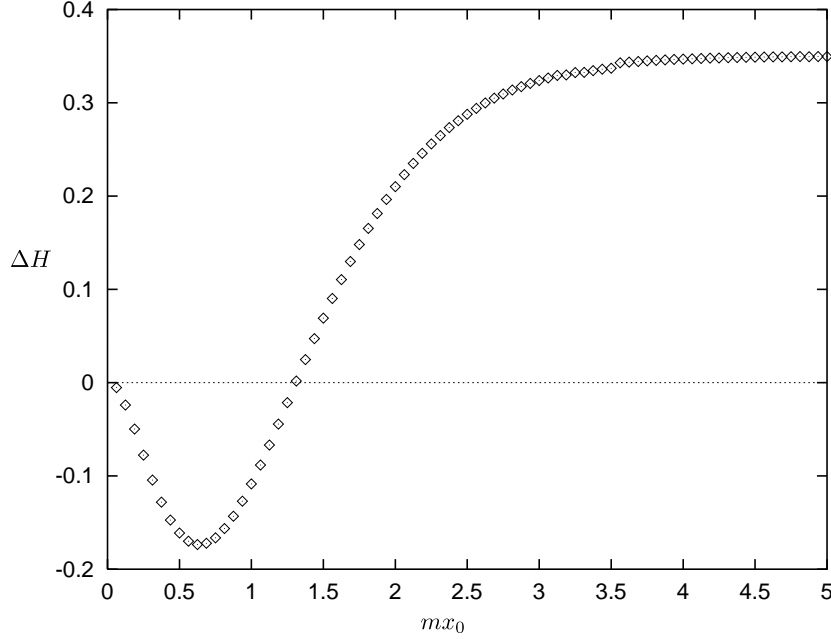


Figure 3-4: One-loop fermionic correction to the energy as a function of  $x_0$  in units of  $m$ .

Fig. 3-4 shows the values of  $\mathcal{E}[\phi_0]$  we obtain from eq. (3.13) as a function of  $x_0$ . In the  $x_0 \rightarrow \infty$  limit, we can also do the calculation analytically. We will expand on this technique in our discussion of the supersymmetric case below. We find a phase shift

$$\delta_F(k) = 4 \tan^{-1} \frac{m}{2k} + 2 \tan^{-1} \frac{m}{k} \quad (3.17)$$

with Born approximation

$$\delta_F^{(1)}(k) = \frac{4m}{k} \quad (3.18)$$

and contributions from two bound states at  $\omega = m\frac{\sqrt{3}}{2}$  and one at  $\omega = m$ . We thus find

$$\mathcal{E}[\phi_0] = 2m \left( \frac{1}{\pi} - \frac{1}{4\sqrt{3}} \right) \quad (3.19)$$

which agrees with the numerical calculation.

# Chapter 4

## The supersymmetric model in one dimension

Having analyzed bosons and fermions separately, we now combine these results and consider the full supersymmetric model in one dimension. Here we will work analytically using a general potential, with the  $\phi^4$  and sine-Gordon theories providing two concrete examples. The supersymmetric model also introduces another quantity, the central charge, which we must also compute in order to check the consistency of our results for the energy. A review of the literature shows a wide variety of conflicting results[8, 12, 13, 9, 14, 15]. Our techniques for dealing with the regularization, renormalization and calculation of one-loop corrections to the energies of classical field configurations will enable us to take a fresh look at this problem. We will obtain an unambiguous result for the energy and the central charge, and in the process we will see how our techniques are related to the expansion of the quantum field in creation and annihilation operators.

### 4.1 Formalism

We begin with the classical supersymmetric Lagrangian density in 1+1 dimensions

$$\mathcal{L} = \frac{m^2}{2\lambda} \left( (\partial_\mu \phi)(\partial^\mu \phi) - U(\phi)^2 + i\bar{\Psi}\not{\partial}\Psi - U'(\phi)\bar{\Psi}\Psi \right) \quad (4.1)$$

where  $\phi$  is a real scalar,  $\Psi$  is a Majorana fermion, and  $U(\phi) = \frac{m}{2}(\phi^2 - 1)$  for the  $\phi^4$  model and  $U(\phi) = 2m \sin(\phi/2)$  for the sine-Gordon model. These models support classical soliton and antisoliton solutions, which are the solutions to

$$\phi'_0(x) = \mp U(\phi_0) \quad (4.2)$$

for the soliton and antisoliton respectively. In the  $\phi^4$  model, the soliton solution is the “kink” that we have already discussed,

$$\phi_0^{\text{kink}}(x) = \tanh \frac{mx}{2}, \quad (4.3)$$

while the soliton in the sine-Gordon model is given by

$$\phi_0^{\text{SG}}(x) = 4 \tan^{-1} e^{-mx}, \quad (4.4)$$

and in both cases the antisoliton is obtained from the soliton by sending  $x \rightarrow -x$ .

The eigenvalue equations for the bosonic and fermionic small oscillations are

$$\left( -\frac{d^2}{dx^2} + U'(\phi_0)^2 + U(\phi_0)U''(\phi_0) \right) \eta_k(x) = (\omega_k^B)^2 \eta_k(x) \quad (4.5)$$

$$\gamma^0 \left( -i\gamma^1 \frac{d}{dx} + U'(\phi_0) \right) \psi_k(x) = \omega_k^F \psi_k(x). \quad (4.6)$$

The bosonic potentials are given by

$$U'(\phi_0)^2 + U(\phi_0)U''(\phi_0) - m^2 = - \left( \frac{\ell + 1}{\ell} \right) m^2 \text{sech}^2 \frac{mx}{\ell} \equiv V_\ell(x) \quad (4.7)$$

with  $\ell = 1$  for the sine-Gordon soliton and  $\ell = 2$  for the kink. Repeating our results from above, we have phase shifts

$$\begin{aligned} \delta_B^{\text{kink}}(k) = \delta_{\ell=2}(k) &= 2 \tan^{-1} \left( \frac{3mk}{2k^2 - m^2} \right) \\ \delta_B^{\text{SG}}(k) = \delta_{\ell=1}(k) &= 2 \tan^{-1} \frac{m}{k} \end{aligned} \quad (4.8)$$

and bound states at  $\omega = 0$  for the kink  $\omega = \frac{\sqrt{3}m}{2}$ , and at  $\omega = 0$  for the sine-Gordon soliton. As discussed above, both potentials have half-bound states at threshold, a necessary consequence of their reflectionless property.

As above, we avoid subtleties of boundary conditions by computing the fermionic phase shifts for a widely separated soliton and antisoliton solution, with the antisoliton on the left so that  $U'(\phi) \rightarrow m$  as  $x \rightarrow \pm\infty$ . We will use the second-order equation obtained by squaring eq. (4.6),

$$\begin{pmatrix} -\frac{d^2}{dx^2} + V_\ell(x) & 0 \\ 0 & -\frac{d^2}{dx^2} + \tilde{V}_\ell(x) \end{pmatrix} \psi_k(x) = k^2 \psi_k(x) \quad (4.9)$$

for the soliton and

$$\begin{pmatrix} -\frac{d^2}{dx^2} + \tilde{V}_\ell(x) & 0 \\ 0 & -\frac{d^2}{dx^2} + V_\ell(x) \end{pmatrix} \psi_k(x) = k^2 \psi_k(x) \quad (4.10)$$

for the antisoliton, where  $\tilde{V}_\ell(x) = \frac{1}{\ell^2} V_{\ell-1}(\frac{x}{\ell})$ . An incident wave far to the left is given by

$$\psi_k(x) = e^{ikx} \begin{pmatrix} 1 \\ ie^{i\theta} \end{pmatrix} \quad (4.11)$$

with  $\theta = \tan^{-1} \frac{k}{m}$ . To start with, we will restrict to the case of a reflectionless potential, such as the kink or sine-Gordon soliton. It thus scatters without reflection through the antisoliton becoming

$$\psi_k(x) = e^{ikx} \begin{pmatrix} e^{i\tilde{\delta}_\ell} \\ ie^{i(\delta_\ell + \theta)} \end{pmatrix} \quad (4.12)$$

where  $\delta_\ell(k)$  is the phase shift for the bosonic potential  $V_\ell(x)$  and  $\tilde{\delta}_\ell(k)$  is the phase shift for the bosonic potential  $\tilde{V}_\ell(x)$ . It then scatters without reflection through the soliton giving

$$\psi_k(x) = e^{ikx} \begin{pmatrix} e^{i(\tilde{\delta}_\ell + \delta_\ell)} \\ ie^{i(\tilde{\delta}_\ell + \delta_\ell + \theta)} \end{pmatrix}. \quad (4.13)$$



By rescaling the results from Appendix A, we easily obtain

$$\tilde{\delta}_\ell(k) = \delta_\ell(k) - 2 \tan^{-1} \frac{m}{k} \quad (4.14)$$

so that for the soliton/antisoliton pair,

$$\delta_F(k) = \delta_B(k) - 2 \tan^{-1} \frac{m}{k} \quad (4.15)$$

and thus for a single soliton

$$\delta_F(k) = \delta_B(k) - \tan^{-1} \frac{m}{k} \quad (4.16)$$

in both models. This result has been also been obtained in [13] and [9]. Through this analysis, we see that the deficit between the boson and fermion phase shifts is necessary so that eq. (4.12) correctly solves the Dirac equation in the region where  $V_F(x) = -m$ . This result also agrees with the methods of the previous section.

These results generalize to any supersymmetric potential  $U(\phi)$  that supports a soliton  $\phi_0$  with  $\phi_0(x) = -\phi_0(-x)$ . We can still consider eq. (4.9), with  $V_\ell(x)$  and  $\tilde{V}_\ell(x)$  replaced by

$$V(x) = U'(\phi_0)^2 + U(\phi_0)U''(\phi_0) - m^2 \quad (4.17)$$

and

$$\tilde{V}(x) = U'(\phi_0)^2 - U(\phi_0)U''(\phi_0) - m^2. \quad (4.18)$$

These are symmetric, though now not necessarily reflectionless, bosonic potentials. We decompose their solutions into symmetric and antisymmetric channels. For  $x \rightarrow \pm\infty$ , these solutions are given in terms of phase shifts as

$$\begin{aligned} \eta_k^S(x) &= \cos(kx \pm \delta^S(k)) & \eta_k^A(x) &= \sin(kx \pm \delta^A(k)) \\ \tilde{\eta}_k^S(x) &= i \cos(kx \pm \tilde{\delta}^S(k)) & \tilde{\eta}_k^A(x) &= -i \sin(kx \pm \tilde{\delta}^A(k)) \end{aligned} \quad (4.19)$$

where the arbitrary factors of  $\pm i$  are inserted for convenience later. For all  $x$  these

wavefunctions are related by

$$\begin{aligned}
\omega_k \tilde{\eta}_k^S(x) &= i \left( \frac{d}{dx} + U'(\phi_0) \right) \eta_k^A(x) & \omega_k \eta_k^A(x) &= i \left( \frac{d}{dx} - U'(\phi_0) \right) \tilde{\eta}_k^S(x) \\
\omega_k \tilde{\eta}_k^A(x) &= i \left( \frac{d}{dx} + U'(\phi_0) \right) \eta_k^S(x) & \omega_k \eta_k^S(x) &= i \left( \frac{d}{dx} - U'(\phi_0) \right) \tilde{\eta}_k^A(x)
\end{aligned}
\tag{4.20}$$

so that the solutions to the Dirac equation are

$$\psi_k^+(x) = \begin{pmatrix} \eta_k^S \\ \tilde{\eta}_k^A \end{pmatrix} \quad \text{and} \quad \psi_k^-(x) = \begin{pmatrix} \eta_k^A \\ \tilde{\eta}_k^S \end{pmatrix} \tag{4.21}$$

with positive and negative parity respectively. The phase relation between the upper and lower components of these wavefunctions must be different as  $x \rightarrow \pm\infty$  since the mass term has opposite signs in these two limits.

Putting this all together gives, as  $x \rightarrow \pm\infty$ ,

$$\begin{aligned}
\cos(kx \pm \delta^S(k)) &= \frac{1}{\omega_k} \left( \frac{d}{dx} - V_F(x) \right) \sin(kx \pm \tilde{\delta}^A(k)) \\
&= \frac{1}{\omega_k} \left( k \cos(kx \pm \tilde{\delta}^A(k)) \mp m \sin(kx \pm \tilde{\delta}^A(k)) \right) \\
&= \mp \sin(kx \pm \tilde{\delta}^A(k) \mp \theta) = \cos(kx \pm \tilde{\delta}^A(k) \mp \theta \pm \frac{\pi}{2}) \tag{4.22}
\end{aligned}$$

and thus

$$\delta^S(k) = \tilde{\delta}^A(k) + \tan^{-1} \frac{m}{k} \tag{4.23}$$

and similarly

$$\delta^A(k) = \tilde{\delta}^S(k) + \tan^{-1} \frac{m}{k}. \tag{4.24}$$

The fermion phase shift in each channel is given by the average of the bosonic phase shifts of the two components

$$\begin{aligned}
\delta^+(k) &= \frac{1}{2}(\delta^S(k) + \tilde{\delta}^A(k)) = \delta^S(k) - \frac{1}{2} \tan^{-1} \frac{m}{k} \\
\delta^-(k) &= \frac{1}{2}(\delta^A(k) + \tilde{\delta}^S(k)) = \delta^A(k) - \frac{1}{2} \tan^{-1} \frac{m}{k}
\end{aligned}
\tag{4.25}$$

so that

$$\delta_F(k) = \delta^+(k) + \delta^-(k) = \delta^S(k) + \delta^A(k) - \tan^{-1} \frac{m}{k} \quad (4.26)$$

and we obtain the same result, eq. (4.16), as we found in the reflectionless case.

Since  $\delta_F(0) \neq \delta_B(0)$ , Levinson's theorem requires that the spectrum of fermionic and boson bound states differ. The difference is that, although there is a fermionic bound state for every bosonic bound state, the mode at  $\omega = 0$  only counts as  $\frac{1}{2}$  for the fermions. (The fermionic states at threshold also count as  $\frac{1}{2}$ , the same as in the boson case.) We have seen this difference in the previous section by tracking the bound state energies as we interpolated between the trivial vacuum and a soliton/antisoliton pair. We can also check this result analytically by observing that the residue of the pole at  $k = im$  in the reflection coefficient  $\mathcal{T}_F$  is half the residue of the pole at  $k = im$  in  $\mathcal{T}_B$  because of eq. (4.16). As a final check, we imagine doubling the spectrum by turning  $\phi$  into a complex scalar and  $\Psi$  into a Dirac fermion. Then in a soliton background  $\phi$  would have two zero-energy bound states, one involving its real part and one involving its imaginary part. However,  $\Psi$  would have only a single zero-energy bound state, with wavefunction given by

$$\psi(x) = \begin{pmatrix} e^{-\int_0^x V_F(y) dy} \\ 0 \end{pmatrix} \quad (4.27)$$

with  $V_F(x) = U'(\phi_0)$ . The corresponding solution with only an lower component is not normalizable; for an antisoliton, we would find the same situation with upper and lower components reversed. Thus when we reduce to a Majorana fermion, we count this state as a half.

We note that the fermionic phase shift and bound state spectrum are simply given by the average of the results we would obtain for the two bosonic potentials  $V_\ell(x)$  and  $\tilde{V}_\ell(x)$ . We also note that just as the bosonic zero mode arises because the soliton breaks translation invariance, the fermionic zero mode arises as a consequence of broken supersymmetry invariance (which we can think of as breaking translation invariance in a fermionic direction in superspace). For a soliton solution, only the

supersymmetry generator  $Q_-$  is broken, while  $Q_+$  is left unbroken (the situation is reversed for an antisoliton). Thus since the supersymmetry is only half broken, it is not surprising that the corresponding zero mode counts only as a half. In both cases, acting with the broken generator on the soliton solution gives the corresponding zero mode.

## 4.2 Applications

To compute the one-loop correction to the energy, we now follow the same method as in the previous sections and sum the quantity  $\frac{1}{2}\omega$  over bosonic and fermionic states, with the fermions entering with a minus sign as usual. We will discuss the case of an isolated soliton, and see that results agree with the widely separated soliton/antisoliton pair considered in the last section.

Thus our formal expression for the energy correction is

$$\Delta H = \frac{1}{2} \sum_j \omega_j^B - \frac{1}{2} \sum_j \omega_j^F + \int_0^\infty \frac{dk}{2\pi} \omega \left( \frac{d\delta_B}{dk} - \frac{d\delta_F}{dk} \right) \quad (4.28)$$

where the states at threshold and the fermion bound state at  $\omega = 0$  are weighted by  $\frac{1}{2}$  as discussed above. The free density of states has cancelled between bosons and fermions, as required by supersymmetry. Again, to avoid infrared problems later, we use Levinson's theorem

$$\delta(0) = \pi(n_B - \frac{1}{2}) \quad (4.29)$$

to rewrite eq. (4.28) as

$$\Delta H = \frac{1}{2} \sum_j (\omega_j^B - m) - \frac{1}{2} \sum_j (\omega_j^F - m) + \int_0^\infty \frac{dk}{2\pi} (\omega - m) \left( \frac{d\delta_B}{dk} - \frac{d\delta_F}{dk} \right) \quad (4.30)$$

where the  $\frac{1}{2}$  in eq. (4.29) has cancelled between bosons and fermions.

The continuum integral in eq. (4.30) is still logarithmically divergent at large  $k$ , as we should expect since we have not yet included the contribution from the counterterm. As above, we can isolate this divergence in the contributions from the

low order Born approximations to the phase shifts  $\delta_B$  and  $\delta_F$ . We then identify these contributions with specific Feynman graphs, subtract the Born approximations, and add back in the associated graphs. For the boson, the divergence comes from the first Born approximation, which corresponds exactly to the tadpole graphs with a bosonic loop. For the fermion, the source of the divergence is more complicated: we subtract the first Born approximation to the fermionic phase shift and the piece of the second Born approximation that is related to it by the spontaneous symmetry breaking of  $\phi$ . This subtraction corresponds exactly to subtracting the tadpole graph with a fermionic loop and the part of the graph with two external bosons and a fermionic loop that is related to the tadpole graph by spontaneous symmetry breaking (the rest of the two-point function is then finite). For both the boson and fermion, this subtraction amounts to simply subtracting the term proportional to  $\frac{1}{k}$  that cancels the leading  $\frac{1}{k}$  behavior of the phase shift at large  $k$ . We can identify the coefficient of these  $\frac{1}{k}$  terms with the coefficients of the logarithmic divergences in the corresponding diagrams. As a result, by computing the divergences in the bosonic and fermionic diagrams, we obtain a check on eq. (4.16), to leading order in  $\frac{1}{k}$  for  $k$  large.

Of course we must add back all that we have subtracted, together with the contribution from the counterterm. To do so we must consider renormalization. We will continue to use our simple renormalization scheme, in which we introduce only the subtraction

$$\mathcal{L} \rightarrow \mathcal{L} - CU''(\phi)U(\phi) - CU'''(\phi)\bar{\Psi}\Psi \quad (4.31)$$

which is equivalent to

$$U(\phi) \rightarrow U(\phi) + \frac{\lambda}{m^2}CU''(\phi) \quad (4.32)$$

and thus preserves supersymmetry. We fix the coefficient  $C$  by requiring that the boson tadpole (which includes contributions from both boson and fermion loops as we have described above) vanish. In this scheme, the counterterm completely cancels the terms we have subtracted from eq. (4.30), so there is nothing to add back in. In the sine-Gordon theory, this scheme also makes the physical mass of the boson equal to  $m$ , while in the  $\phi^4$  theory, there is a one-loop correction to the physical mass of

the boson from the diagram with two three-boson vertices, giving a physical mass of  $m - \frac{\lambda}{4m\sqrt{3}}$  [9]. For us it is more important to guarantee that the tadpole graphs vanish, assuring us that we have chosen the correct vacuum for the theory, than to have the physical mass equal to the Lagrangian parameter  $m$ ; for the sine-Gordon case we happen to be able to do both at once. Furthermore, such renormalization conditions can be applied uniformly to arbitrary  $U(\phi)$ .

Thus the effect of regularization and renormalization in our renormalization scheme is to subtract

$$\delta^{(1)}(k) = \delta_B^{(1)}(k) - \delta_F^{(1)}(k) = \frac{m}{k} \quad (4.33)$$

from the difference of the boson and fermion phase shifts, giving

$$\begin{aligned} \Delta H &= \frac{1}{2} \sum_j (\omega_j^B - m) - \frac{1}{2} \sum_j (\omega_j^F - m) \\ &\quad + \int_0^\infty \frac{dk}{2\pi} (\omega - m) \left( \frac{d\delta_B}{dk} - \frac{d\delta_F}{dk} - \frac{d\delta^{(1)}}{dk} \right) \\ &= -\frac{m}{4} + \int_0^\infty \frac{dk}{2\pi} (\omega - m) \frac{d}{dk} \left( \tan^{-1} \frac{m}{k} - \frac{m}{k} \right) = -\frac{m}{2\pi} \end{aligned} \quad (4.34)$$

for both the kink and sine-Gordon soliton. This result agrees with [9] and [14], and disagrees with [12], [8], [13], and [15]. As pointed out in [9], in the case of the sine-Gordon soliton, it also agrees with the result obtained from the Yang-Baxter equation assuming the factorization of the S-matrix [17].

We note that in the end this result depended only on eq. (4.16) and its implications for Levinson's theorem. Thus, since eq. (4.16) holds in general for antisymmetric soliton solutions, eq. (4.34) gives the one-loop correction to the energy in our renormalization scheme of any supersymmetric soliton that is antisymmetric under reflection.

### 4.3 Supersymmetry algebra and the central charge

Our second application of the apparatus we have developed is to compute the one-loop quantum correction to the central charge in the presence of the kink or sine-Gordon

soliton.

First we summarize the supersymmetry algebra. We define

$$Q_{\pm} = \frac{(1 \mp i\gamma^1)}{2} \frac{m^2}{\lambda} \int (\not{\partial}\phi + iU)\gamma^0\Psi \, dx = \frac{m^2}{\lambda} \int (\Pi\Psi_{\pm} + (\phi' \pm U)\Psi_{\mp}) \, dx \quad (4.35)$$

where  $\Psi_{\pm} = \frac{1 \mp i\gamma^1}{2}\Psi$  and  $Q_{\pm} = \frac{1 \mp i\gamma^1}{2}Q$ . Using the canonical equal-time (anti)commutation relations, we have

$$\begin{aligned} \frac{m^2}{\lambda} \{i\Psi_{\pm}(x), \Psi_{\pm}(y)\} &= i\delta(x-y) \\ \frac{m^2}{\lambda} [\phi(x), \Pi(y)] &= i\delta(x-y) \end{aligned} \quad (4.36)$$

where  $\Pi = \dot{\phi}$  is the momentum conjugate to  $\phi$  and all other (anti)commutators vanish. The supersymmetry algebra is

$$\{Q_{\pm}, Q_{\pm}\} = 2H \pm 2Z \quad \{Q_+, Q_-\} = 2P, \quad (4.37)$$

where  $H$ ,  $P$ , and  $Z$  are given classically by

$$\begin{aligned} H &= \frac{m^2}{2\lambda} \int \left( \Pi^2 + (\phi')^2 + U^2 + i(\Psi_-\Psi'_+ + \Psi_+\Psi'_-) + 2iU'\Psi_-\Psi_+ \right) dx \\ P &= \frac{m^2}{\lambda} \int \left( \Pi\phi' + \frac{i}{2}(\Psi_+\Psi'_+ + \Psi_-\Psi'_-) \right) dx \\ Z &= \frac{m^2}{\lambda} \int \phi'U \, dx. \end{aligned} \quad (4.38)$$

It is easy to check that  $H$  is the same Hamiltonian as would be determined canonically from eq. (4.1).

At the classical level, using eq. (4.2),

$$H_{\text{cl}} = \frac{m^2}{2\lambda} \int \left( \phi'_0(x)^2 + U(\phi_0)^2 \right) dx = \mp \frac{m^2}{\lambda} \int U(\phi_0(x))\phi'_0(x) = \mp Z_{\text{cl}}, \quad (4.39)$$

for the soliton and antisoliton respectively.

The hermiticity of  $Q_{\pm}$  gives the BPS bound on the expectation values of  $H$  and

$Z$  in any quantum state:

$$\langle H \rangle \geq |\langle Z \rangle|. \quad (4.40)$$

Classically, the values of  $H$  and  $|Z|$  are equal so this bound is saturated. We have found a negative correction to  $H$  at one-loop, so if there is no correction to  $Z$ , eq. (4.40) will be violated.

To unambiguously compute the corrections to the central charge for a soliton, it is easier to consider corrections to  $Q_+^2 = H + Z$ , which is zero classically (for the antisoliton we should consider  $Q_-^2 = H + Z$ ). One reason to consider  $Q_+^2$  rather than  $H$  and  $Z$  separately is that this quantity is finite and independent of the renormalization scheme. Using eq. (4.31) and eq. (4.32) we see explicitly that the contribution from the counterterm cancels:

$$\Delta H_{\text{ct}} = C \int U''(\phi_0) U(\phi_0) dx = -C \int U''(\phi_0) \phi_0' dx = -\Delta Z_{\text{ct}} \quad (4.41)$$

(and we only need consider the tree-level contribution since the counterterm coefficient  $C$  is already order  $\lambda^0$ ).

Next we expand  $\phi(x) = \phi_0(x) + \eta(x)$ , where the soliton solution  $\phi_0$  is an ordinary real function of  $x$ . Neglecting terms of order  $\eta^3$  and higher (which give higher-loop corrections), we obtain

$$\begin{aligned} \langle H + Z \rangle_\phi = & \frac{m^2}{2\lambda} \int \left\langle \Pi^2 + \left[ \left( \frac{d}{dx} + U'(\phi_0) \right) \eta \right]^2 \right. \\ & + i\Psi_+ \left( \frac{d}{dx} - U'(\phi_0) \right) \Psi_- \\ & \left. + i\Psi_- \left( \frac{d}{dx} + U'(\phi_0) \right) \Psi_+ \right\rangle_\phi dx, \end{aligned} \quad (4.42)$$

where  $\langle \rangle_\phi$  denotes expectation value in the classical soliton background.

To evaluate this expression, we decompose the fields  $\eta$  and  $\Psi$  using creation and annihilation operators for the small oscillations around  $\phi_0$ . The small oscillation modes will be given in terms of the eigenmodes of the bosonic potentials  $V_\ell(x)$  and  $\tilde{V}_\ell(x) = \frac{1}{\ell^2} V_{\ell-1}(\frac{x}{\ell})$ . For any mode  $\eta_k(x)$  of  $V_\ell(x)$  with nonzero energy  $\omega_k = \sqrt{k^2 + m^2}$ ,



there is a mode  $\tilde{\eta}_k(x)$  of  $\tilde{V}_\ell(x)$  with the same energy, related by

$$\begin{aligned}\omega_k \tilde{\eta}_k(x) &= i \left( \frac{d}{dx} + U'(\phi_0) \right) \eta_k \\ \omega_k \eta_k(x) &= i \left( \frac{d}{dx} - U'(\phi_0) \right) \tilde{\eta}_k.\end{aligned}\tag{4.43}$$

We use these wavefunctions to obtain

$$\begin{aligned}\eta(x) &= \sqrt{\frac{\lambda}{m^2}} \int \frac{dk}{\sqrt{4\pi\omega_k}} \left( a_k \eta_k(x) e^{-i\omega_k t} + a_k^\dagger \eta_k^*(x) e^{i\omega_k t} \right) \\ &\quad + \sqrt{\frac{\lambda}{m^2}} \eta_{\omega=0}(x) a_{\omega=0} \\ \Psi(x) &= \sqrt{\frac{\lambda}{m^2}} \int \frac{dk}{\sqrt{4\pi\omega_k}} \left( b_k \psi_k(x) e^{-i\omega_k t} + b_k^\dagger \psi_k^*(x) e^{i\omega_k t} \right) \\ &\quad + \sqrt{\frac{\lambda}{m^2}} \psi_{\omega=0}(0) b_{\omega=0}\end{aligned}\tag{4.44}$$

where  $\eta_{-k}(x) = \eta_k^*(x)$ , the creation and annihilation operators obey

$$[a_k, a_{k'}^\dagger] = \{b_k, b_{k'}^\dagger\} = \delta(k - k')\tag{4.45}$$

with all other (anti)commutators vanishing, and

$$\psi_k(x) = \sqrt{\omega_k} \begin{pmatrix} \eta_k(x) \\ \tilde{\eta}_k(x) \end{pmatrix}.\tag{4.46}$$

We note that the integral over  $k$  also includes discrete contributions from the bound states (which correspond to imaginary values of  $k$ ). These are understood to give discrete contributions to the results that follow (with Dirac delta functions replaced by Kronecker delta functions appropriately). However, we have explicitly indicated the contribution from the bound states at  $\omega = 0$  following [18].

We normalize the wavefunctions  $\eta_k$  such that

$$\int \frac{dk}{2\pi} \eta_k(x)^* \eta_k(y) = \delta(x - y)\tag{4.47}$$

which implies

$$\int \frac{dk}{2\pi} \tilde{\eta}_k(x)^* \tilde{\eta}_k(y) = \delta(x - y). \quad (4.48)$$

With this normalization, the fields  $\eta$  and  $\Psi$  obey canonical commutation relations.

Elementary algebra yields

$$\begin{aligned} i \left( \frac{d}{dx} + U'(\phi_0) \right) \eta &= \sqrt{\frac{\lambda}{m^2}} \int \frac{dk \sqrt{\omega_k}}{\sqrt{4\pi}} \left( a_k \tilde{\eta}_k(x) e^{-i\omega_k t} - a_k^\dagger \tilde{\eta}_k(x)^* e^{i\omega_k t} \right) \\ i\Pi &= \sqrt{\frac{\lambda}{m^2}} \int \frac{dk \sqrt{\omega_k}}{\sqrt{4\pi}} \left( a_k \eta_k(x) e^{-i\omega_k t} - a_k^\dagger \eta_k(x)^* e^{i\omega_k t} \right) \\ \Psi_+ &= \sqrt{\frac{\lambda}{m^2}} \int \frac{dk}{\sqrt{4\pi}} \left( b_k \eta_k(x) e^{-i\omega_k t} + b_k^\dagger \eta_k(x)^* e^{i\omega_k t} \right) \\ &\quad + \sqrt{\frac{\lambda}{m^2}} \eta_{\omega=0}(x) b_{\omega=0} \\ \Psi_- &= \sqrt{\frac{\lambda}{m^2}} \int \frac{dk}{\sqrt{4\pi}} \left( b_k \tilde{\eta}_k(x) e^{-i\omega_k t} + b_k^\dagger \tilde{\eta}_k(x)^* e^{i\omega_k t} \right) \\ i \left( \frac{d}{dx} + U'(\phi_0) \right) \Psi_+ &= \sqrt{\frac{\lambda}{m^2}} \int \frac{\omega_k dk}{\sqrt{4\pi}} \left( b_k \tilde{\eta}_k(x) e^{-i\omega_k t} - b_k^\dagger \tilde{\eta}_k(x)^* e^{i\omega_k t} \right) \\ i \left( \frac{d}{dx} - U'(\phi_0) \right) \Psi_- &= \sqrt{\frac{\lambda}{m^2}} \int \frac{\omega_k dk}{\sqrt{4\pi}} \left( b_k \eta_k(x) e^{-i\omega_k t} - b_k^\dagger \eta_k(x)^* e^{i\omega_k t} \right) \end{aligned} \quad (4.49)$$

and we find

$$\begin{aligned} \langle H + Z \rangle_\phi &= \int dx \int \frac{dk}{8\pi} \omega_k |\eta_k(x)|^2 + \int dx \int \frac{dk}{8\pi} \omega_k |\tilde{\eta}_k(x)|^2 \\ &\quad - \int dx \int \frac{dk}{8\pi} \omega_k |\tilde{\eta}_k(x)|^2 - \int dx \int \frac{dk}{8\pi} \omega_k |\eta_k(x)|^2 = 0 \end{aligned} \quad (4.50)$$

and the BPS bound remains saturated. (If we instead considered an antisoliton, we would find the same result for  $\langle Q_-^2 \rangle_{\bar{\phi}} = \langle H - Z \rangle_{\bar{\phi}}$ , with the roles of  $\Psi_+$  and  $\Psi_-$  reversed.) Our result disagrees with [9] and [15], which claim that there is no correction to the central charge at one loop in this renormalization scheme. We note that this result did not depend on any specific properties of  $U$ , so it holds for any supersymmetric soliton satisfying eq. (4.2).

The second line of eq. (4.50) is simply the unregulated fermionic contribution to the energy, and is explicitly equal to minus the average of the contributions from the bosonic potentials  $V_\ell$  and  $\tilde{V}_\ell$ , in agreement with what we found above. As a

final consistency check, we recalculate the full one-loop correction to the energy and central charge using our expansion in terms of quantum fields. For  $\Delta H$  we obtain, again neglecting  $\eta^3$  terms,

$$\begin{aligned}
\Delta H &= \langle H \rangle_\phi - H_{\text{cl}} \\
&= \frac{m^2}{2\lambda} \int \left\langle \Pi^2 + \eta \left( -\frac{d^2}{dx^2} + U'(\phi_0)^2 + U(\phi_0)U''(\phi_0) \right) \eta \right. \\
&\quad \left. + i\Psi_+ \left( \frac{d}{dx} - U'(\phi_0) \right) \Psi_- + i\Psi_- \left( \frac{d}{dx} + U'(\phi_0) \right) \Psi_+ \right\rangle_\phi dx \\
&= \Delta H_{\text{ct}} \\
&\quad + \int dx \int \frac{dk}{4\pi} \omega_k |\eta_k(x)|^2 - \int dx \int \frac{dk}{8\pi} \omega_k (|\tilde{\eta}_k(x)|^2 + |\eta_k(x)|^2). \quad (4.51)
\end{aligned}$$

To relate this expression to our phase shift formalism, we consider the Green's function for the bosonic field

$$\begin{aligned}
G(x, y, t) &= iT \langle \eta(x, t) \eta(y, 0) \rangle \\
&= i \int \frac{dk}{4\pi\omega_k} \left( e^{i\omega_k t} \eta_k^*(x) \eta_k(y) \Theta(t) \right. \\
&\quad \left. + e^{-i\omega_k t} \eta_k(x) \eta_k^*(y) \Theta(-t) \right) \quad (4.52)
\end{aligned}$$

and its Fourier transform

$$G(x, y, \omega) = \int G(x, y, t) e^{i\omega t} dt = \int \frac{dk}{2\pi} \left( \frac{\eta_k(x) \eta_k^*(y)}{\omega^2 - \omega_k^2 - i\epsilon} \right) \quad (4.53)$$

whose trace gives the density of states according to

$$\rho_B(\omega) = \text{Im} \frac{2\omega}{\pi} \int G(x, x, \omega) dx \quad (4.54)$$

giving as a result

$$\rho_B(k) = \frac{1}{\pi} \int dx |\eta_k(x)|^2. \quad (4.55)$$

Similarly for the fermions we find

$$\rho_F(k) = \frac{1}{2\pi} \int dx (|\eta_k(x)|^2 + |\tilde{\eta}_k(x)|^2). \quad (4.56)$$

These results enable us to verify that eq. (4.51) is in agreement with eq. (4.34).

In the exact same way, we can calculate the correction to  $Z$  directly. We start from the classical expression for  $Z$  in eq. (4.38) and expand about the classical solution  $\phi = \phi_0$ , giving

$$\begin{aligned}
\Delta Z &= \langle Z \rangle_\phi - Z_{\text{cl}} \\
&= \Delta Z_{\text{ct}} + \frac{m^2}{\lambda} \int \left\langle U' \eta \eta' - \frac{1}{2} U U'' \eta^2 \right\rangle_\phi dx \\
&= \Delta Z_{\text{ct}} + \frac{m^2}{2\lambda} \int \left\langle \left( \left( \frac{d}{dx} + U' \right) \eta \right)^2 - (\eta')^2 - \eta^2 (U')^2 - U U'' \eta^2 \right\rangle_\phi dx. \quad (4.57)
\end{aligned}$$

After substituting the expansions of eq. (4.49) we obtain

$$\begin{aligned}
\Delta Z &= \Delta Z_{\text{ct}} + \int dx \int \frac{dk}{8\pi} \omega_k |\tilde{\eta}_k(x)|^2 - \int dx \int \frac{dk}{8\pi} \omega_k |\eta_k(x)|^2 \\
&= \frac{1}{4} \sum_j (\tilde{\omega}_j - m) - \frac{1}{4} \sum_j (\omega_j - m) \\
&\quad + \int \frac{dk}{4\pi} (\omega_k - m) \frac{d}{dk} \left( \tilde{\delta}_l(k) - \delta_l(k) + 2\delta^{(1)}(k) \right) \\
&= \frac{m}{4} - \int \frac{dk}{2\pi} (\omega - m) \frac{d}{dk} \left( \tan^{-1} \frac{m}{k} - \frac{m}{k} \right) = \frac{m}{2\pi} = -\Delta H. \quad (4.58)
\end{aligned}$$

Another work [20] has explained the difference between our result for the central charge and the result obtained in Ref. [9] and predecessors. The earlier works found  $\Delta Z = 0$  based on an argument that involves direct manipulation of the  $Z$  operator. However, Ref. [20] showed that manipulations of this type are only valid if the operator is augmented with an anomalous correction of order  $\hbar$ .

We have systematically avoided the questionable manipulations that would have led to  $\Delta Z = 0$  by computing only matrix elements, where we have the phase shift formalism available to guide us. First we developed an unambiguous renormalization procedure for  $H$  based on physical quantities. Classical BPS saturation defines the operator  $Z$  at tree level. Once we have fixed a renormalization scheme in our computation of  $H$ , the expectation value of  $Z$  (or any other physical quantity) is determined. We then carried out the one-loop computation of  $Z$  exactly in parallel to the computation of  $H$  so that no new ambiguities could arise, and found that BPS

saturation is maintained at one loop, as confirmed in Ref. [20]. Our use of Levinson's theorem and the Born approximation also prevented the appearance of the spurious linear divergences found in Ref. [9].

Thus we consistently included the effects of the SVV anomaly in both  $H$  and  $Z$ , though of course we found only a particular matrix element instead of the full operator. However, by working in the continuum (without boundaries), we avoided the difficulties that Ref. [20] faced in separating the unphysical contributions at the boundaries from the physical effects localized at the soliton.

# Chapter 5

## Scalars in three dimensions

Having fully analyzed models in one dimension, we now turn to three dimensions. We will continue to consider models with spherical symmetry, so that we can use a partial wave decomposition. Thus, in addition to an integral over  $k$ , we will also have a sum over  $\ell$  to consider. On the other hand, the subtleties of the symmetric channel in one dimension will be absent. Theories in three dimensions will also have stronger divergences than we found in one dimension. Thus we will have to subtract more Born terms and add back in more corresponding diagrams. However, since all the theories we will consider are renormalizable, only a finite number of Born subtractions will be required. We will again begin with a scalar model, but our techniques will easily generalize to include fermions.

### 5.1 Formalism

We consider a renormalizable field theory with a real scalar field  $\phi$  coupled to a charged scalar  $\Psi$ . We take the classical potential  $V(\phi) \propto (\phi^2 - v^2)^2$ , and  $\Psi$  acquires a mass through spontaneous symmetry breaking. At the quantum level we put aside the  $\phi$  self-couplings and consider only the effects of the  $\phi - \Psi$  interactions. We further restrict ourselves to  $\mathcal{O}(\hbar)$  effects in the quantum theory, which correspond to one-loop diagrams.

Our model is defined by the classical action

$$S[\phi, \Psi] = \int d^4x \left\{ \frac{1}{2}(\partial_\mu \phi)^2 - \frac{\lambda}{4!}(\phi^2 - v^2)^2 + \partial_\mu \Psi^* \partial^\mu \Psi - g \Psi^* \phi^2 \Psi \right. \\ \left. + a(\partial_\mu \phi)^2 - b(\phi^2 - v^2) - c(\phi^2 - v^2)^2 \right\} ,$$

where we have separated out the three counterterms necessary for renormalization and written them in a convenient form. At one-loop order in  $\Psi$ , these are the only counterterms required.

We quantize around the classical vacuum  $\phi = v$  and define  $h = \phi - v$ , so that

$$S[h, \Psi] = \int d^4x \left\{ \frac{1}{2}(\partial_\mu h)^2 - \frac{m^2}{8v^2}(h^2 + 2vh)^2 - g(h^2 + 2vh)\Psi^* \Psi \right. \\ \left. + \partial_\mu \Psi^* \partial^\mu \Psi - M^2 \Psi^* \Psi \right. \\ \left. + a(\partial_\mu h)^2 - b(h^2 + 2hv) - c(h^2 + 2hv)^2 \right\}$$

where  $M = \sqrt{g}v$  is the  $\Psi$  mass and  $m^2 = \lambda v^2/3$  is the  $h$  mass.

The one-loop quantum effective action for  $h$  is obtained by integrating out  $\Psi$  to leading order in  $\hbar$ . We are interested in time-independent field configurations  $h = h(\vec{x})$ , for which the effective action yields an effective energy  $\mathcal{E}[h]$  that has three parts:

$$\mathcal{E}[h] = \mathcal{E}_{\text{cl}}[h] + \mathcal{E}_{\text{ct}}[h] + \mathcal{E}_\Psi[h] , \quad (5.1)$$

where  $\mathcal{E}_{\text{cl}}[h]$  is the classical energy of  $h$ ,

$$\mathcal{E}_{\text{cl}}[h] = \int d^3x \left\{ \frac{1}{2}|\vec{\nabla} h|^2 + \frac{m^2}{8v^2}(h^2 + 2vh)^2 \right\} , \quad (5.2)$$

$\mathcal{E}_{\text{ct}}[h]$  is the counterterm contribution,

$$\mathcal{E}_{\text{ct}}[h] = \int d^3x \left\{ a|\vec{\nabla} h|^2 + b(h^2 + 2hv) + c(h^2 + 2hv)^2 \right\} , \quad (5.3)$$

and  $\mathcal{E}_\Psi[h]$  is the one-loop quantum contribution from  $\Psi$ .  $\mathcal{E}_{\text{ct}}[h]$  and  $\mathcal{E}_\Psi[h]$  are divergent, but we will see explicitly that these divergences cancel for any configuration  $h(\vec{x})$ .

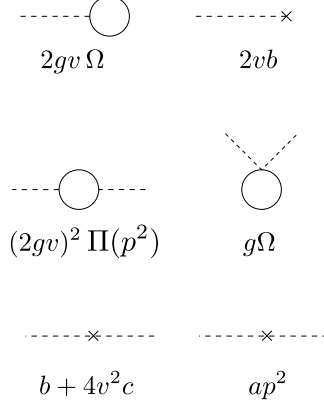


Figure 5-1: One-loop diagrams.

We fix the counterterms by applying renormalization conditions in the perturbative sector of the theory. Having done so, we have defined the theory for all  $h(\vec{x})$ . We choose the on-shell renormalization conditions

$$\Sigma_1 = 0, \quad \Sigma_2(m^2) = 0, \quad \text{and} \quad \left. \frac{d\Sigma_2}{dp^2} \right|_{m^2} = 0, \quad (5.4)$$

where  $\Sigma_1$  and  $\Sigma_2(p^2)$  are the one- and two-point functions arising only from the loop and counterterms as seen in Fig. 5-1. We denote the one-loop diagrams with one insertion by  $\Omega$  and with two insertions by  $\Pi(p^2)$ , and find

$$\begin{aligned} \Sigma_1 &= 2vg\Omega + 2vb, \\ \Sigma_2(p^2) &= (2vg)^2\Pi(p^2) + g\Omega + b + (2v)^2c + ap^2. \end{aligned} \quad (5.5)$$

Defining

$$\Pi'(p^2) \equiv \frac{d\Pi(p^2)}{dp^2}, \quad (5.6)$$

the renormalization conditions eq.(5.4) then yield

$$a = -(2vg)^2\Pi'(m^2), \quad b = -g\Omega, \quad c = g^2(m^2\Pi'(m^2) - \Pi(m^2)), \quad (5.7)$$

which we then substitute into the counterterm energy, eq. (5.3).

Now we consider the calculation of  $\mathcal{E}_\Psi[h]$ . This energy is the sum over zero point



energies,  $\frac{1}{2}\hbar\omega$ , of the modes of  $\Psi$  in the presence of  $h(\vec{x})$ ,

$$\mathcal{E}_\psi[h] = \sum_\alpha \omega_\alpha[h] \quad (5.8)$$

where  $\omega_k$  are the positive square roots of the eigenvalues of the small oscillations Hamiltonian,

$$\left(-\vec{\nabla}^2 + M^2 + g(h^2 + 2vh)\right) \psi_k = \omega_\alpha^2 \psi_k \quad (5.9)$$

The fact that  $\Psi$  is complex accounts for the absence of  $\frac{1}{2}$  in eq. (5.8).

$\mathcal{E}_\Psi$  is highly divergent. However our model is renormalizable and therefore the counterterms fixed in the presence of the trivial  $h$  *must* cancel all divergences in  $\mathcal{E}_\Psi$ . Rather than attempt to regulate the divergent sum in eq. (5.8) directly, we study the density of states that defines the sum. We can isolate the terms that lead to divergences in  $\mathcal{E}_\Psi$  and renormalize them using conventional methods. Thus our task is to generalize the construction of eq. (2.7) to this case.

For fixed  $h(\vec{x})$  the spectrum of  $\hat{H}$  given in eq. (5.9) consists of a finite number (possibly zero) of normalizable bound states and a continuum beginning at  $M^2$ , parameterized by  $k$ , with  $E(k) = +\sqrt{k^2 + M^2}$ . Furthermore,  $\hat{H}$  depends on  $h$  only through the combination

$$\chi = h^2 + 2hv, \quad (5.10)$$

so we can consider  $\mathcal{E}_\Psi$  to be a functional of  $\chi$ . We restrict ourselves to spherically symmetric  $h$ . Then

$$\mathcal{E}_\Psi[\chi] = \sum_j E_j + \sum_\ell (2\ell + 1) \int dk \rho_\ell(k) E(k) \quad (5.11)$$

where  $\rho_\ell(k)$  is the density of states in  $k$  in the  $\ell^{\text{th}}$  partial wave and the  $E_j$  are the bound state energies.  $\rho_\ell(k)$  is finite, but the sum over  $\ell$  and the integral over  $k$  are divergent. Furthermore

$$\rho_\ell(k) = \rho_\ell^{\text{free}}(k) + \frac{1}{\pi} \frac{d\delta_\ell(k)}{dk}, \quad (5.12)$$

where  $\delta_\ell(k)$  is the usual scattering phase shift for the  $\ell^{\text{th}}$  partial wave, and  $\rho_\ell^{\text{free}}(k)$  is

the free ( $g = 0$ ) density of states. This relationship between the density of states and the derivative of the phase shift is shown for example in [14].

At the outset, we subtract  $\rho^{\text{free}}(k)$  from the density of states since we wish to compare  $\mathcal{E}_\Psi[\chi]$  to  $\mathcal{E}_\Psi[0]$ . Viewing  $\mathcal{E}_\Psi[\chi]$  as the sum of one loop diagrams, we see that only the diagrams with one or two insertions of  $g\chi$  are divergent. A diagram with  $n$  insertions corresponds to the  $n^{\text{th}}$  term in the Born expansion, so all possible divergences can be eliminated by subtracting the first and second Born approximations from the phase shifts that determine the density of states. Standard methods allow us to construct the Born approximation for the phase shifts [6], which is a power series in the “potential”  $g\chi$ .

We define the combination

$$\bar{\delta}_\ell(k) \equiv \delta_\ell(k) - \delta_\ell^{(1)}(k) - \delta_\ell^{(2)}(k) , \quad (5.13)$$

where  $\delta_\ell^{(1)}(k)$  and  $\delta_\ell^{(2)}(k)$  are the first and second Born approximations to  $\delta_\ell(k)$ . We then have

$$\begin{aligned} \mathcal{E}_\Psi[\chi] = & \sum_j E_j + \sum_\ell (2\ell + 1) \int_0^\infty dk \frac{1}{\pi} \frac{d\bar{\delta}_\ell(k)}{dk} E(k) + g\Omega \int \frac{d^3p}{(2\pi)^3} \tilde{\chi}(0) \\ & + g^2 \int \frac{d^3p}{(2\pi)^3} \Pi(-\vec{p}^2) |\tilde{\chi}(\vec{p})|^2 \end{aligned} \quad (5.14)$$

where

$$\tilde{\chi}(\vec{p}) = \int d^3x \chi(\vec{x}) e^{-i\vec{p}\cdot\vec{x}} , \quad (5.15)$$

and likewise for  $\tilde{h}(\vec{p})$ . Both  $\tilde{h}$  and  $\tilde{\chi}$  are real and depend only on  $q \equiv |\vec{p}|$  for spherically symmetric  $h$ . We have subtracted out the order  $g$  and  $g^2$  contributions by using  $\bar{\delta}_\ell(k)$  instead of  $\delta_\ell(k)$ , and added them back in by using their explicit diagrammatic representation in terms of the divergent constant  $\Omega$  and the divergent function  $\Pi(p^2)$ .

We can now combine  $\mathcal{E}_\Psi$  and  $\mathcal{E}_{\text{ct}}$  and obtain a finite result:

$$\mathcal{E}_\Psi + \mathcal{E}_{\text{ct}} = \sum_j E_j + \sum_\ell (2\ell + 1) \int_0^\infty dk \frac{1}{\pi} \frac{d\bar{\delta}_\ell(k)}{dk} E(k) + \Gamma_2[h] \quad (5.16)$$

where

$$\begin{aligned}\Gamma_2[h] &= \frac{g^2}{2} \int_0^\infty \frac{q^2 dq}{2\pi^2} \left[ \left( \Pi(-q^2) - \Pi(m^2) + m^2 \Pi'(m^2) \right) \tilde{\chi}(q)^2 \right] \\ &\quad + \frac{g^2}{2} \int_0^\infty \frac{q^2 dq}{2\pi^2} \left[ 4v^2 q^2 \Pi'(-q^2) \tilde{h}(q)^2 \right].\end{aligned}\quad (5.17)$$

$\Pi$  is log divergent, but both  $\{\Pi(-q^2) - \Pi(m^2)\}$  and  $\Pi'$  are finite, so  $\Gamma_2[h]$  is finite as well.

Each term in the Born approximation to the phase shift goes to zero at  $k = 0$ , so by Levinson's theorem  $\bar{\delta}_\ell(0) = \delta_\ell(0) = \pi n_\ell$  where  $n_\ell$  is the number of bound states with angular momentum  $\ell$ . As  $k \rightarrow \infty$ ,  $\delta_\ell(k)$  falls off like  $\frac{1}{k}$ ,  $\delta_\ell^{(1)}(k)$  falls off like  $\frac{1}{k}$ , and  $\delta_\ell^{(2)}(k)$  falls off like  $\frac{1}{k^2}$ . Since the Born approximation becomes exact at large  $k$ ,  $\bar{\delta}_\ell(k)$  falls like  $\frac{1}{k^3}$ . Thus we see that the first subtraction renders each integral over  $k$  convergent. The second subtraction makes the  $\ell$ -sum convergent. We are then free to integrate by parts in (5.16), obtaining

$$\mathcal{E}[h] = \mathcal{E}_{\text{cl}}[h] + \Gamma_2[h] - \frac{1}{\pi} \sum_\ell (2\ell + 1) \int_0^\infty dk \bar{\delta}_\ell(k) \frac{k}{E(k)} + \sum_j (E_j - M). \quad (5.18)$$

In this expression we see that each bound state contributes its binding energy,  $E_j - M$ , so that the energy varies smoothly as we strengthen  $h$  and bind more states.

## 5.2 Computational methods

In this Section we describe the method that allows us to construct  $\mathcal{E}[h]$  as a functional of  $h$  and search for stationary points. We now consider the calculation of each of the terms in eq. (5.18) in turn. The classical contribution to the action is evaluated directly by substitution into eq. (5.2).  $\Gamma_2[h]$  of eq. (5.17) is obtained from a Feynman diagram calculation,

$$\begin{aligned}\Gamma_2[h] &= \frac{g^2}{(4\pi)^2} \int_0^\infty \frac{q^2 dq}{(2\pi)^2} \int_0^1 \left[ \log \frac{M^2 + q^2 x(1-x)}{M^2 - m^2 x(1-x)} \right. \\ &\quad \left. - \frac{m^2 x(1-x)}{M^2 - m^2 x(1-x)} \right] \tilde{\chi}(q)^2 dx\end{aligned}$$

$$-\frac{g^2}{(4\pi)^2} \int_0^\infty \frac{q^2 dq}{(2\pi)^2} \int_0^1 \left[ \frac{x(1-x)}{M^2 - m^2 x(1-x)} 4v^2 q^2 \tilde{h}(q)^2 \right] dx. \quad (5.19)$$

The partial wave phase shifts and Born approximations are calculated as follows. The radial wave equation is

$$-u_\ell'' + \left[ \frac{\ell(\ell+1)}{r^2} + g\chi(r) \right] u_\ell = k^2 u_\ell, \quad (5.20)$$

where  $k^2 > 0$ , and  $\chi(r) \rightarrow 0$  as  $r \rightarrow \infty$ . We introduce two linearly independent solutions to eq. (5.20),  $u_\ell^{(1)}(r)$  and  $u_\ell^{(2)}(r)$ , defined by

$$\begin{aligned} u_\ell^{(1)}(r) &= e^{2i\beta_\ell(k,r)} r h_\ell^{(1)}(kr) \\ u_\ell^{(2)}(r) &= e^{-2i\beta_\ell^*(k,r)} r h_\ell^{(2)}(kr) \end{aligned} \quad (5.21)$$

where  $h_\ell^{(1)}$  is the spherical Hankel function asymptotic to  $e^{ikr}/r$  as  $r \rightarrow \infty$ ,  $h_\ell^{(2)}(kr) = h_\ell^{(1)*}(kr)$ , and  $\beta_\ell(k, r) \rightarrow 0$  as  $r \rightarrow \infty$ , so that  $u_\ell^{(1)}(r) \rightarrow e^{ikr}$  and  $u_\ell^{(2)}(r) \rightarrow e^{-ikr}$  as  $r \rightarrow \infty$ . The scattering solution is then

$$u_\ell(r) = u_\ell^{(2)}(r) + e^{2i\delta_\ell(k)} u_\ell^{(1)}(r), \quad (5.22)$$

and obeys  $u_\ell(0) = 0$ . Thus we obtain

$$\delta_\ell(k) = -2 \operatorname{Re} \beta_\ell(k, 0). \quad (5.23)$$

Furthermore,  $\beta_\ell$  obeys a simple, non-linear differential equation obtained by substituting  $u_\ell^{(1)}$  into eq. (5.20),

$$-i\beta_\ell'' - 2ikp_\ell(kr)\beta_\ell' + 2(\beta_\ell')^2 + \frac{1}{2}g\chi(r) = 0, \quad (5.24)$$

where primes denote differentiation with respect to  $r$ , and

$$p_\ell(x) = \frac{d}{dx} \ln [x h_\ell^{(1)}(x)] \quad (5.25)$$

is a simple rational function of  $x$ .

We solve eq. (5.24) numerically, integrating from  $r = \infty$  to  $r = 0$  with  $\beta'_\ell(k, \infty) = \beta_\ell(k, \infty) = 0$ , to get the exact phase shifts. To get the Born approximation to  $\beta_\ell$ , we solve the equation iteratively, writing  $\beta_\ell = g\beta_{\ell 1} + g^2\beta_{\ell 2} + \dots$ , where  $\beta_{\ell 1}$  satisfies

$$-i\beta''_{\ell 1} - 2ikp_\ell(kr)\beta'_{\ell 1} + \frac{1}{2}\chi(r) = 0 \quad (5.26)$$

and  $\beta_{\ell 2}$  satisfies

$$-i\beta''_{\ell 2} - 2ikp_\ell(kr)\beta'_{\ell 2} + 2(\beta'_{\ell 1})^2 = 0. \quad (5.27)$$

We can solve efficiently for  $\beta_{\ell 1}$  and  $\beta_{\ell 2}$  simultaneously by combining these two equations into a coupled differential equation for the vector  $(\beta_{\ell 1}, \beta_{\ell 2})$ . This method is much faster than calculating the Born terms directly as iterated integrals in  $r$  and will generalize easily to a theory requiring higher-order counterterms.

Having found the phase shifts, we then use Levinson's theorem to count bound states. We then find the energies of these bound states by using a shooting method to solve the corresponding eigenvalue equation. We use the effective range approximation [6] to calculate the phase shift and bound state energy near the threshold for forming an s-wave bound state.

## 5.3 Results

For the model at hand, we calculated the energy  $\mathcal{E}[h]$  for a two-parameter ( $d$  and  $w$ ) family of Gaussian backgrounds

$$h(r) = -dve^{-r^2v^2/2w^2} . \quad (5.28)$$

In Fig. 5-2, we show results which are representative of our findings in general. We plot the energy of configurations with fixed  $d = 1$  as a function of  $w$ , for  $g = 1, 2, 4, 8$  (from top to bottom). We note that to this order, for  $g = 8$  the vacuum is unstable to the formation of large  $\phi = 0$  regions.

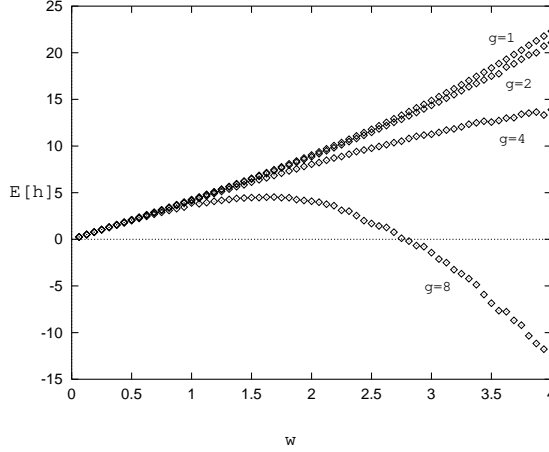


Figure 5-2:  $\mathcal{E}[h]$  in units of  $v$ , for  $d = 1$  and  $g = 1, 2, 4, 8$ , as a function of  $w$ .

To explore whether the charged scalar forms a non-topological soliton in a given  $\phi$  background, we add to  $\mathcal{E}[h]$  the energy of a “valence”  $\Psi$  particle in the lowest bound state. We then compare this total energy to  $M$ , the energy of the  $\Psi$  particle in a flat background, to see if the soliton is favored. This is the scalar model analog of  $t$ -quark bag formation.

For fixed  $g$  and  $m$ , we varied  $h$  looking for bound states with energy  $E$  such that  $E + \mathcal{E}[h] < M$ . However, for those values of  $g$  and  $m$  where we did find such solutions, we always found that by increasing  $w$ , we could make  $\mathcal{E}[h] < 0$ , so that the vacuum is unstable, as we pointed out above in the case of  $g = 8$  in Fig. 5-2. Thus we find that if we stay in the  $g, m$  parameter region where the vacuum is stable, the minimum is at  $h = 0$ , so there are no nontopological solitons.

Although we did not find a non-trivial solution at one-loop order in this simple model, our calculation demonstrates the practicality of our method in three dimensions. We can effectively characterize and search the space of field configurations,  $h(r)$ , while holding the renormalized parameters of the theory fixed. The same methods can be used to study solitons in theories with richer structure in three dimensions.

## 5.4 Derivative expansion

Our results are exact to one-loop order. The derivative expansion, which is often applied to problems of this sort, should be accurate for slowly varying  $h(r)$ . We found it useful to compare our results with the derivative expansion for two reasons: first, we can determine the range of validity (in  $d$  and  $w$ ) of the derivative expansion; and second, where the derivative expansion is expected to be valid, it provides a check on the accuracy of our numerical work and C++ programming. Where expected, the two calculations did agree to the precision we specified (1 %).

In our model, the first two terms in the derivative expansion of the one-loop effective Lagrangian can be calculated to be

$$\mathcal{L}_1 = \mathcal{L}_{\text{ct}} + \alpha z + \beta z^2 + \frac{g^2 v^4}{32\pi^2} \left[ (1+z)^2 \ln(1+z) - z - \frac{3}{2} z^2 \right] + \frac{g}{48\pi^2 v^2} \frac{1}{1+z} (\partial_\mu z)^2, \quad (5.29)$$

where  $z = g\chi/M^2 = (h^2 + 2hv)/v^2$ ,  $\alpha$  and  $\beta$  are cutoff-dependent constants, and  $\mathcal{L}_{\text{ct}}$  is the same counterterm Lagrangian as we used in Sec. 2. For  $\phi^4$  scalar field theory a similar result was first derived in [5]. The last term above is proportional to  $(\partial h)^2$ , and is completely cancelled by a finite counterterm that implements the renormalization prescription of Sec. 2. In this prescription, counterterms also cancel the  $\alpha z$  and  $\beta z^2$  terms above. Thus the  $\mathcal{O}(p^2)$  derivative expansion for the effective energy, to be compared with the phase shift expression for  $\mathcal{E}[h]$ , is

$$\begin{aligned} \mathcal{E}_{\text{DE}}[h] = \int d^3x \left\{ \frac{(\vec{\nabla} h)^2}{2} + \frac{m^2}{8v^2} (h^2 + 2hv)^2 \right. \\ \left. + \frac{g^2 v^4}{32\pi^2} \left[ (1+z)^2 \ln(1+z) - z - \frac{3}{2} z^2 \right] \right\}. \end{aligned} \quad (5.30)$$

The results of the comparison with the phase shift method can be seen in Fig. 5-3 for  $d = 0.25$ , and  $g = 4$ . A similar pattern holds in general for other values of both  $d$  and  $g$ . As the width becomes larger, the two results merge. This is as expected, since it is for large widths, and thus small gradients, that we expect the derivative

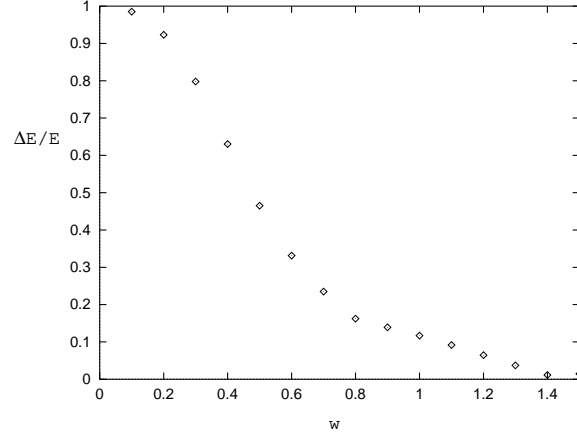


Figure 5-3:  $|(\mathcal{E} - \mathcal{E}_{\text{DE}})/(\mathcal{E} - \mathcal{E}_{\text{cl}})|$  for  $d = 0.25$ ,  $g = 4$ , as a function of  $w$ .

expansion to yield accurate results. As the width tends to zero, both results tend to zero, and the fact that the plot tends to 1 simply indicates that the derivative expansion result goes to zero faster than the phase shift result.



# Chapter 6

## Fermions in three dimensions

It is now an easy matter to extend these three dimensional results to fermions. We continue to consider a classical background  $\phi$ , now coupled to a Dirac fermion  $\Psi$ . Our Lagrangian becomes

$$\begin{aligned}\mathcal{L} = & \frac{1}{2}(\partial_\mu\phi)^2 - \frac{\lambda}{4!}(\phi^2 - v^2)^2 + i\bar{\psi}\not{\partial}\psi - g\phi\bar{\psi}\psi \\ & + a(\partial_\mu\phi)^2 - b(\phi^2 - v^2) - c(\phi^2 - v^2)^2 \quad .\end{aligned}\tag{6.1}$$

The small oscillations are now given by the Dirac equation,

$$\gamma^0 \left( -i\gamma^i \partial_i + m + gh \right) \psi_k = \omega \psi_k \tag{6.2}$$

where  $h = \phi - v$  and  $m = gv$ . We will continue to work with a symmetric background  $h$ , so we can decompose our small oscillations into channels according to angular momentum.

Letting  $\alpha^i = \gamma^0 \gamma^i$  and  $\beta = \gamma^0$ , we will work in the basis

$$\alpha^k = \begin{pmatrix} 0 & \sigma_k \\ \sigma_k & 0 \end{pmatrix} \quad \text{and} \quad \beta = \begin{pmatrix} 1 & 0 \\ 0 & -1 \end{pmatrix} \tag{6.3}$$

where the  $\sigma_k$  are the standard Pauli matrices. We define the operator

$$Q = \beta(\vec{\sigma} \cdot \vec{L}) \quad (6.4)$$

where  $\vec{L} = \vec{r} \times \vec{p}$ . This operator commutes with the Hamiltonian, and is related to the total angular momentum operator  $\vec{J} = \vec{L} + \frac{1}{2}\vec{\sigma}$  by  $Q^2 = \vec{J}^2 + \frac{1}{4}$ . We can thus restrict to states with a particular eigenvalue  $q$  of the operator  $Q$ , with  $q = \pm 1, \pm 2, \pm 3 \dots$ . We also introduce the radial momentum operator

$$p_r = -i \left( \frac{d}{dr} + \frac{1}{r} \right) \quad (6.5)$$

which allows us to rewrite eq. (6.2) as

$$\left( \alpha_r p_r + \frac{i}{r} \alpha_r \beta q + \beta(m + gh(r)) \right) \psi_k = \omega \psi_k \quad (6.6)$$

where  $\alpha_r = \hat{r} \cdot \vec{\alpha}$ . The solutions to this equation will be of the form

$$\psi_k^+ = \frac{1}{r} \begin{pmatrix} F(r) \mathcal{Y}_{(q-1)j}^M \\ iG(r) \mathcal{Y}_{qj}^M \end{pmatrix} \quad (6.7)$$

for  $q > 0$  and

$$\psi_k^- = \frac{1}{r} \begin{pmatrix} F(r) \mathcal{Y}_{|q|j}^M \\ -iG(r) \mathcal{Y}_{(|q|-1)j}^M \end{pmatrix} \quad (6.8)$$

for  $q < 0$ , where  $\mathcal{Y}_{\ell j}^M$  is the two-component spinor spherical harmonic corresponding to a state with total angular momentum  $j$ , orbital angular momentum  $\ell$ , and a  $z$  component of angular momentum  $M$ . These two solutions are eigenstates of parity with eigenvalues  $\pm(-1)^q$  respectively. The functions  $F$  and  $G$  obey the coupled radial equations

$$\begin{aligned} ((\omega - m) - gh(r)) F + \frac{dG}{dr} + \frac{q}{r} G &= 0 \\ ((\omega + m) + gh(r)) G - \frac{dF}{dr} + \frac{q}{r} F &= 0. \end{aligned} \quad (6.9)$$

If we set  $h(r) = 0$ ,  $F$  and  $G$  obey the second-order equations

$$\begin{aligned} \left( -\frac{d^2}{dr^2} + \frac{q(q-1)}{r^2} \right) F &= k^2 F \\ \left( -\frac{d^2}{dr^2} + \frac{q(q+1)}{r^2} \right) G &= k^2 G \end{aligned} \quad (6.10)$$

where  $\omega = \sqrt{k^2 + m^2}$ . Thus the free solutions for  $F$  and  $G$  will be spherical harmonics  $j_\ell(kr)$ , with  $\ell$  equal to the orbital angular momentum of the spherical harmonic that the radial function multiplies in eq. (6.7) or eq. (6.8).

In each channel, it is convenient to work with the full second-order equation that we obtain by squaring the Dirac equation. Any solution to the Dirac equation must solve this equation as well, and if we choose our boundary conditions so that the Dirac equation is solved, a solution to the second-order equation will automatically solve the Dirac equation. To facilitate our numerical computation, we will focus on the upper component, since its equation will involve the quantity  $\omega + m$  rather than  $\omega - m$ , and the former is easier to deal with numerically at small  $k$ . (The small  $k$  limit is also the nonrelativistic limit, and in this limit the upper component is large compared to the lower component, which makes it easier to deal with numerically; if we were investigating negative energy solutions it would be easier to use the lower component.) We will therefore label our channels by parity (as above) and by  $\ell = 0, 1, 2, \dots$ , the orbital angular momentum of the upper component. The total spin  $j$  is then equal to  $\ell + \frac{1}{2}$  for positive parity and  $\ell - \frac{1}{2}$  for negative parity. (Only positive parity exists for  $\ell = 0$ .)

Plugging  $F(r) = e^{2i\beta(r)} r h_\ell^{(1)}(kr)$  into the full second-order equation for  $F$  gives

$$-i\beta_\ell^{+''} - 2ikp_\ell(kr)\beta_\ell^{+'} + 2(\beta_\ell^{+'})^2 + \frac{1}{2} \left( g^2\chi + g \frac{h'(r)(kp_\ell(kr) - \frac{\ell+1}{r} + i\beta_\ell^{+'})}{(E + m + gh(r))} \right) = 0 \quad (6.11)$$

in the positive parity channel, and

$$-i\beta_\ell^{-''} - 2ikp_\ell(kr)\beta_\ell^{-'} + 2(\beta_\ell^{-'})^2 + \frac{1}{2} \left( g^2\chi + g \frac{h(r)'(kp_\ell(kr) + \frac{\ell}{r} + i\beta_\ell^{-'})}{(E + m + gh(r))} \right) = 0 \quad (6.12)$$

in the negative parity channel. As in the bosonic case, we have defined

$$\chi = h^2 + 2hv. \quad (6.13)$$

Again, the phase shift is given by

$$\delta_\ell^\pm(k) = -2 \operatorname{Re} \beta_\ell^\pm(k, 0). \quad (6.14)$$

We also have stronger divergences than in the bosonic case, so we must subtract the first four terms in the Born approximation and add them back in as diagrams. As a result, the numerical computation is somewhat more complicated; nonetheless, the basic method is the same: we iterate the differential equations for the phase shifts to obtain the Born approximations, which again cancel the divergences at large  $k$  and  $\ell$  (though for small  $k$  and  $\ell$ , the Born approximation may deviate widely from the exact phase shift). As in the boson model, the Born approximations to the phase shift go to zero at  $k = 0$ , while the exact phase shifts go to  $\pi$  times the number of bound states in that channel. And, as we would expect, there is an overall Fermi minus sign in front of the entire result.

This computation adds the full Casimir energy to the computation of [22]; as indicated above, to consistently compute the effect of the shift in the valence quark level requires that we include the Casimir energy as well. However, in this model, although the quantitative results are modified, the qualitative conclusions for moderate values of  $g$  are unchanged.

An interesting generalization of this model is to add isospin, making the background field into a complex 2-component vector. We can then construct “hedgehog” configurations that have nontrivial topology. These configurations are no longer  $CP$  invariant. In particular, they can have spectral asymmetry, which is reflected by a fermion level crossing during the process of adiabatically constructing the configuration from the trivial vacuum. If a level crossing does occur, the configuration carries fermion number and we do not need to fill an energy level at all. Even if a level crossing does not occur, the level that is heading toward zero is often strongly bound

and thus costs only a small amount of energy.

To consider configurations that violate  $CP$ , we must address the question of whether to sum the quantity  $-\frac{1}{2}|\omega|$  over all modes or the quantity  $\omega$  the negative modes. (If  $C$  or  $CP$  is not broken, the two methods give the same answer.) The former shows more consistency with the boson computation, while the latter is what one would expect from a Dirac sea picture, since the negative modes are the ones that are filled. The first method is correct. One can prove this formally [21], but here we will show it via a simple example, ordinary QED. Consider QED with a massive fermion, and imagine turning on a very weak, slowly varying electric field. To leading order in the coupling, this field will shift both positive and negative energy levels in the same direction, with corresponding particle and antiparticle states being shifted by the same amount. If we were to sum only the shifts in the negative energy levels, we would find a divergent result at the leading order in the Born approximation. However, there is no available counterterm to cancel this infinity. If instead we calculate the shift summing all of the levels, to first order we simply get zero, since the shifts in the particle states cancel against the shift in the antiparticle states. This result agrees with the loop calculation, where we find that the leading contribution is identically zero, with no contribution from the counterterm. (Note that this result is different from what we find to leading order for scalar field. In that case, the particle and antiparticle levels move toward zero, and both sums give the same divergent result. However, in this case there is a counterterm available to cancel out this divergence.)

A hedgehog configuration breaks rotational invariance, but we can choose it to stay within the spherical ansatz, so that it is invariant under grand spin (simultaneous rotations in physical space and isospin space). We decompose the spectrum into a sum over channels labeled by their grand spin and their parity. Each channel now has two coupled degrees of freedom instead of one, but still can be described by a second-order (matrix) differential equation. Summing the two eigenphases gives us the total contribution to the density of states from that channel. This matrix equation must also be iterated through fourth order to obtain the Born approximations corresponding to the divergent diagrams.

Calculation in this generalized model in principle requires no further modifications to the framework presented above. However, there are practical difficulties associated with the increased computational complexity. Even in the model without isospin, the third- and fourth- order diagrams involve multidimensional integrals over external momenta and Feynman parameters. One possible simplification is to use a “toy” boson model with the same divergence structure as the third- and fourth-order diagrams. If chosen properly, this model will exhibit the same local at second order as the fermions have at third and fourth order, so subtracting its second-order phase shifts and adding back in its second-order diagram (in the fermionic renormalization scheme, of course) can regulate the theory in a computationally simpler way. Such a manipulation is possible only because the divergences are simple, local functions of the background field; the finite parts of the bosonic diagram will of course be very different from the finite parts of the fermionic diagrams. However, because we add back in everything we have subtracted, using counterterms fixed in the fermion theory, we have not changed the final answer. Work is underway on this model [23].

# Chapter 7

## Conclusions

We have seen that the continuum density of states formalism has allowed us to apply the powerful calculational tools of quantum mechanics — phase shifts, Born approximations and Levinson’s theorem — to nontrivial problems in quantum field theory. These formal tools provide the robust framework we need to do unambiguous calculations. Without them, we could have easily missed the subtleties of bosonic and fermionic spectra that we have seen above, and such a mistake would lead to a drastic change in the end result. Such errors are intolerable because of their theoretical consequences, as in the case of the saturation of the BPS bound in 1+1 dimensional supersymmetric theories, and because of their phenomenological consequences, as in the case of heavy quark “bags” in the Standard Model.

One can envision many other applications of this work. As mentioned above, the most immediate is to include fermions coupled to scalars with isospin in the spherical ansatz. One could also imagine adding gauge fields to such a model, to bring it still closer to the real Standard Model. One could then apply these methods to other gauge theory solitons, such as ’t Hooft-Polyakov monopoles or flux tubes in superconductors. It would also be interesting to see if one could use these techniques to compute quantum corrections to the action of instantons.

# Appendix A: Properties of reflectionless potentials in one dimension

In this section we review the properties of solutions of

$$\left(-\frac{d^2}{dx^2} + V_\ell(x)\right)\eta(x) = k^2\eta(x) \quad (1)$$

with

$$V_\ell(x) = -\ell(\ell+1)m^2\text{sech}^2mx \quad (2)$$

for an integer  $\ell$ . For more details, see [19]. The results used in the soliton problems above will then be obtained by rescaling  $x \rightarrow \frac{x}{\ell}$ . The basic technique will be to define raising and lowering operators

$$\begin{aligned} a_\ell &= i \left( \frac{d}{dx} + \ell m \tanh mx \right) \\ a_\ell^\dagger &= i \left( \frac{d}{dx} - \ell m \tanh mx \right) \end{aligned} \quad (3)$$

so that we can rewrite eq. (1) as

$$(a_\ell^\dagger a_\ell - \ell^2 m^2)\eta(x) = k^2\eta(x) = (a_{\ell+1}^\dagger a_{\ell+1} - (\ell+1)^2 m^2)\eta(x). \quad (4)$$

We can then connect the solutions for a given  $\ell$  with those for  $\ell-1$  by observing that eq. (4) implies that if  $\tilde{\eta}(x)$  is an eigenstate in the potential  $V_{\ell-1}$ , then  $\eta(x) = a_\ell^\dagger \tilde{\eta}(x)$



is an eigenstate in the potential  $V_\ell$  with the same eigenvalue  $k^2$ . Thus we have

$$\begin{aligned}\omega_\ell \tilde{\eta}(x) &= a_\ell \eta(x) \\ \omega_\ell \eta(x) &= a_\ell^\dagger \tilde{\eta}(x)\end{aligned}\tag{5}$$

with  $\omega_\ell = \sqrt{k^2 + \ell^2 m^2}$ . Thus the spectra of  $V_\ell$  and  $V_{\ell-1}$  are identical, except that the spectrum of  $V_\ell$  might contain additional states annihilated by  $a_\ell$ . Indeed, there is exactly one such state, at  $k^2 = -\ell^2 m^2$  (which becomes the zero mode of the corresponding soliton).

By iterating this process, we arrive at  $\ell = 0$ , which is a free particle. Since we know how to solve that problem completely, we can go backwards and solve for any  $V_\ell$  simply by applying raising operators and at each step solving for the one additional zero mode.

For example, for  $\ell = 1$  we start with the free scattering states  $e^{ikx}$  and apply  $a_1^\dagger$ , giving

$$\eta_k^1(x) = \frac{i}{\omega_1} \left( \frac{d}{dx} - m \tanh mx \right) e^{ikx} = -\frac{1}{\omega_1} (k + im \tanh mx) e^{ikx} \tag{6}$$

and a new bound state at  $k^2 = -1$  that satisfies

$$i \left( \frac{d}{dx} + m \tanh mx \right) \eta_0^1(x) = 0 \rightarrow \eta_0^1(k) = \frac{1}{\sqrt{2}} \text{sech} mx. \tag{7}$$

We can then proceed to  $\ell = 2$ , obtaining scattering states

$$\begin{aligned}\eta_k^2(x) &= \frac{i}{\omega_2} \left( \frac{d}{dx} - 2m \tanh mx \right) \eta_k^1(x) \\ &= \frac{1}{\omega_1 \omega_2} ((k + 2im \tanh mx)(k + im \tanh mx) + m^2 \text{sech}^2 mx) e^{ikx} \\ &= \frac{1}{\omega_1 \omega_2} (m^2 + k^2 + 3imk \tanh mx - 3m^2 \tanh^2 mx) e^{ikx}\end{aligned}\tag{8}$$

a bound state at  $k^2 = -1$  given by

$$\eta_1^2(x) = \frac{i}{\sqrt{3}} \left( \frac{d}{dx} - 2m \tanh mx \right) \eta_0^1(x) = -i \sqrt{\frac{3}{2}} \operatorname{sech} mx \tanh mx \quad (9)$$

and a new bound state with  $k^2 = -4$  solving

$$i \left( \frac{d}{dx} + 2m \tanh mx \right) \eta_0^2(x) = 0 \rightarrow \eta_0^2(k) = \sqrt{\frac{3}{4}} \operatorname{sech}^2 mx. \quad (10)$$

We can extend to any integer  $\ell$  by repeating this process. We find that the scattering from these potentials is reflectionless, with phase shift

$$\delta_\ell(k) = 2 \sum_{j=1}^{\ell} \tan^{-1} \left( \frac{jm\ell}{k} \right) \quad (11)$$

and bound states at

$$k^2 = -(mj\ell)^2 \quad (12)$$

for  $j = 0, \dots, \ell$ . The state at  $k^2 = 0$  is a “half-bound” state, right at threshold, which goes to a constant as  $x \rightarrow \pm\infty$ . This state is given by acting with our raising operators on the threshold state in the free case, which is just a constant wavefunction. Thus for  $\ell = 1$  we find

$$\eta_{\text{thresh}}^1 = \frac{i}{m} \left( \frac{d}{dx} - m \tanh mx \right) 1 = -i \tanh mx \quad (13)$$

and for  $\ell = 2$  we obtain

$$\begin{aligned} \eta_{\text{thresh}}^2(x) &= \frac{i}{2m} \left( \frac{d}{dx} - 2m \tanh mx \right) \eta_{\text{thresh}}^1(x) \\ &= \frac{1}{2} (1 - 3 \tanh^2 mx). \end{aligned} \quad (14)$$

We see that in both cases, these states are the  $k \rightarrow 0$  limit of the scattering states, and have the property that they go to a constant (rather than a straight line of some nonzero slope) as  $x \rightarrow \pm\infty$ .

Since  $V_\ell$  is symmetric, we can separate the spectrum of wavefunctions into symmetric and antisymmetric channels. The symmetry of the bound states will alternate, with the lowest energy bound state being symmetric. The phase shift can also be decomposed into contributions from the two channels, with

$$\delta_\ell(k) = \delta_\ell^S(k) + \delta_\ell^A(k). \quad (15)$$

That the scattering is reflectionless is equivalent to

$$\delta_\ell^S(k) = \delta_\ell^A(k). \quad (16)$$

Levinson's theorem for the two channels gives [7]

$$\begin{aligned} \delta_\ell^A(0) &= \pi n_\ell^A \\ \delta_\ell^S(0) &= \pi(n_\ell^S - \frac{1}{2}) \end{aligned} \quad (17)$$

where  $n_\ell^A$  and  $n_\ell^S$  are the numbers of antisymmetric and symmetric bound states in partial wave  $\ell$ , with threshold states counted as one half. Thus we see that the threshold states are essential in reconciling eq. (16) with eq. (17).

# Appendix B: Phase shifts in arbitrary dimensions

In this section we demonstrate explicitly the link between the leading Born approximation to the phase shifts and tadpole diagrams by computing both in dimensional regularization. We consider only the Bose case for simplicity.

In  $n$  spatial dimensions, we consider the bosonic small oscillations in partial wave  $\ell$  with wave number  $k$  in the presence of a  $n$ -dimensionally spherically symmetric bosonic potential  $V(x)$ . As in three dimensions, we can separate variables and obtain a differential for the wavefunction  $\eta(r)$  in partial waves  $\ell$ . Also as in three dimensions, it is convenient to use a rescaled wavefunction  $u = r^{\frac{n}{2}-1}\eta$ , giving a generalized Bessel's equation

$$-\left(\frac{d^2}{dr^2} + \frac{1}{r}\frac{d}{dr} - \frac{1}{r^2}\left(\ell(\ell+n-2) + \left(1 - \frac{n}{2}\right)^2\right)\right)u + Vu = k^2u. \quad (18)$$

This is the same equation as in three dimensions except that the eigenvalue of the Casimir operator  $L^2 = \frac{1}{2}M_{\alpha\beta}M^{\alpha\beta}$  has been generalized from  $\ell(\ell+1)$  to  $\ell(\ell+n-2)$ .

The degeneracy factor for this partial wave (i.e. the dimension of this representation of the rotation group, which gives the generalization of  $2\ell+1$  in three dimensions) is the dimension of the space of symmetric tensors with  $\ell$  indices that each run from 1 to  $n$  with all traces (contractions) removed. Working out the combinatorics gives

$$N_\ell^n = \frac{(n+\ell-1)!}{\ell!(n-1)!} - \frac{(n+\ell-3)!}{(\ell-2)!(n-1)!} \quad (19)$$

which we will analytically continue to arbitrary  $n$  using the gamma function, which satisfies

$$x\Gamma(x) = \Gamma(x+1) \quad \text{and} \quad \Gamma(n+1) = n! \quad (20)$$

For a fuller derivation of eq. (18) and eq. (19) see for example Appendix B of [24].

As we have seen above, the tadpole graph requires the external momentum to be equal to zero. Thus we should expect that both the leading Born approximation and the tadpole graph will depend only on the spatial average of the potential (its  $p = 0$  component),

$$\langle V \rangle = \frac{2\pi^{\frac{n}{2}}}{\Gamma(\frac{n}{2})} \int_0^\infty V(r) r^{n-1} dr. \quad (21)$$

The leading Born approximation to the phase shift is

$$\delta_\ell^{(1)}(k) = -\frac{\pi}{2} \int_0^\infty J_{\frac{n}{2}+\ell-1}(kr)^2 V(r) r dr \quad (22)$$

where  $J_\nu(z)$  is an ordinary Bessel function, related to the spherical Bessel function by  $j_p(z) = \sqrt{\frac{\pi}{2z}} J_{p+\frac{1}{2}}(z)$ . The leading correction to the energy is

$$\mathcal{E}^{(1)} = \sum_{\ell=0}^\infty N_\ell^n \int_0^\infty \frac{dk}{2\pi} (\omega - m) \frac{d\delta_\ell^{(1)}(k)}{dk} \quad (23)$$

where we have used Levinson's theorem as in eq. (2.10). This manipulation was not necessary in our calculations in three dimensions since we did not have any singularities at  $k = 0$ , but it still would have been a perfectly valid thing to do; all the Born approximations vanish at both  $k = 0$  and  $k = \infty$ . However, to calculate in arbitrary dimensions we will need to perform the  $\ell$  sum first. Thus, to avoid the same infrared singularities we saw in one dimension, we again have used Levinson's theorem to add a total derivative to the unregulated integral. As a result, our analysis of arbitrary dimensions will provide further evidence that the correct form of the unregulated sum is indeed that of eq. (2.10).

Using the Bessel function identity

$$\sum_{\ell=0}^{\infty} \frac{(2q+2\ell)(2q+\ell-1)!}{\ell!} J_{q+\ell}(z)^2 = \frac{(2q)!}{(q!)^2} \left(\frac{z}{2}\right)^{2q} \quad (24)$$

we can explicitly do the sum over  $\ell$ , giving

$$\mathcal{E}^{(1)} = -\frac{\langle V \rangle}{(4\pi)^{\frac{n}{2}} \Gamma\left(\frac{n}{2}\right)} \int_0^\infty (\omega - m)(n-2)k^{n-3} dk. \quad (25)$$

The  $k$  integral can be calculated near  $n = \frac{1}{2}$  and then analytically continued, giving

$$\int_0^\infty (\omega - m)k^{n-3} dk = -\frac{m^{n-1}}{4\sqrt{\pi}} \Gamma\left(\frac{1-n}{2}\right) \Gamma\left(\frac{n-2}{2}\right) \quad (26)$$

and so we find

$$\mathcal{E}^{(1)} = \frac{\langle V \rangle}{(4\pi)^{\frac{n+1}{2}}} \Gamma\left(\frac{1-n}{2}\right) m^{n-1} \quad (27)$$

in agreement with what we obtain using standard dimensional regularization of the tadpole diagram in  $n+1$  space-time dimensions.

# Bibliography

- [1] E. D'Hoker and E. Farhi, Nucl. Phys. **B248** (1984) 59, E. D'Hoker and E. Farhi, Nucl. Phys. **B248** (1984) 77
- [2] J. Bagger and S. Naculich, Phys. Rev. Lett. **67** (1991) 2252, Phys. Rev. **D45** (1992) 1395.
- [3] J. Schwinger, Phys. Rev. **94** (1954) 1362. See also W. Greiner, B. Muller and J. Rafelski, *Quantum Electrodynamics of Strong Fields* (Springer, Berlin, 1985).
- [4] E. Farhi, N. Graham, P. Haagenen and R. L. Jaffe, Phys. Lett. **B427** (1998) 334-342, N. Graham and R. L. Jaffe, Phys. Lett. **B435** (1998) 145-151, N. Graham and R. L. Jaffe, Nucl. Phys. **B544** (1999) 432-447, N. Graham and R. L. Jaffe, hep-th/9901023, to appear in Nuclear Physics B.
- [5] S. Coleman, *Aspects of Symmetry* (Cambridge University Press, Cambridge, 1985); (North-Holland, Amsterdam, 1982).
- [6] L. Schiff, *Quantum Mechanics* (McGraw-Hill, NY, 1968).
- [7] G. Barton, J. Phys. A: Math. Gen. **18** (1985) 479.
- [8] A. Rebhan and P. van Nieuwenhuizen, Nucl. Phys. **B508** (1997) 449.
- [9] H. Nastase, M. Stephanov, P. van Nieuwenhuizen and A. Rebhan, Nucl. Phys. **B542** (1999) 471.
- [10] M. Bordag, J. Phys. A: Math. Gen. **28** (1995) 755.

- [11] R. Dashen, B. Hasslacher, and A. Neveu, Phys. Rev. **D10** (1974) 4114, 4130.
- [12] A. d’Adda and P. di Vecchia, Phys. Lett. **73B** (1978) 162; A. d’Adda, R. Horsley and P. di Vecchia, Phys. Lett. **76B** (1978) 298; R. Horsley, Nucl. Phys. **B151** (1979) 399; S. Rouhani, Nucl. Phys. **B182** (1981) 462.; H. Yamagishi, Phys. Lett. **147B** (1984) 425; A. K. Chatterjee and P. Majumdar, Phys. Rev. **D30** (1984) 844; Phys. Lett. **159B** (1985) 37; A. Uchiyama, Nucl. Phys. **B244** (1984) 57; A. Uchiyama, Progr. Theor. Phys. **75** (1986) 1214; A. Uchiyama, Nucl. Phys. **B278** (1986) 121; A. Rebhan and P. van Nieuwenhuizen, Nucl. Phys. **B508** (1997) 449.
- [13] R. K. Kaul and R. Rajaraman, Phys. Lett. **131B** (1983) 357;
- [14] J. F. Schonfeld, Nucl. Phys. **B161** (1979) 125.
- [15] C. Imbimbo and S. Mukhi, Nucl. Phys. **B247** (1984) 471.
- [16] D. Olive and E. Witten, Phys. Lett **78B** (1978) 97.
- [17] K. Schoutens, Nucl. Phys. **B344** (1990) 665; C. Ahn, D. Bernard and A. LeClair, Nucl. Phys. **B246** (1990) 409; C. Ahn, Nucl. Phys. **B354** (1991) 57.
- [18] R. Jackiw and C. Rebbi, Phys. Rev. **D13** (1976) 3398.
- [19] P. Morse and H. Feshbach, *Methods of Mathematical Physics* (McGraw-Hill, New York, 1953).
- [20] M. Shifman, A. Vainshtein and M. Voloshin, Phys. Rev. **D59** (1999) 045016.
- [21] R. Alkofer, H. Reinhardt, and H. Weigel, Phys. Rept. **265** (1996) 139.
- [22] S. Dimopoulos, B. Lynn, S. Selipsky and N. Tetradis, Phys. Lett. **253B** (1991) 237;
- [23] S. Bashinsky, E. Farhi, N. Graham, R. L. Jaffe and H. Weigel, to appear.
- [24] S. Lee, S. Minwalla, M. Rangamani, and N. Seiberg, Adv. Theor. Math. Phys. **2** (1998) 697.